AUTOMATED QRS DETECTION IN THE PRESENCE OF NOISE

by

Isabelle M. Adams

A thesis submitted to the faculty of
The University of Utah
in partial fulfillment of the requirements for the degree of

Master of Science

Department of Medical Biophysics and Computing

The University of Utah

August 1984

THE UNIVERSITY OF UTAH GRADUATE SCHOOL
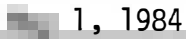
# SUPERVISORY COMMITTEE APPROVAL

of a thesis submitted by

Isabelle M. Adams

This thesis has been read by each member of the following supervisory committee and by majority vote has been found to be satisfactory.

Chairman:

1, 1984

THE UNIVERSITY OF UTAH GRADUATE SCHOOL

FINAL READING APPROVAL

To the Graduate Council of The University of Utah:

I have read the thesis of _____ Isabelle M. Adams _____ in its
final form and have found that (1) its format, citations, and bibliographic style are
consistent and acceptable; (2) its illustrative materials including figures, tables, and
charts are in place; and (3) the final manuscript is satisfactory to the Supervisory
Committee and is ready for submission to the Graduate School.

_____ 1  1984 _____
Date

T. Allan Pryor
Member, Supervisory Committee

Approved for the Major Department

Homer R. Warner
Chairman Dean

Approved for the Graduate Council

ABSTRACT

Accurate QRS detection is essential in on-line computerized
rhythm monitoring systems. A major cause of error in QRS detection
schemes arises from artifacts superimposed on the input signal. To
a lesser extent identification of P or T waves as QRS complexes can
represent another source of error.

In an effort to reduce the incidence of false and missed alarms
generated by the rhythm monitoring system currently used in the LDS
Hospital Coronary Care Unit, a project was undertaken to improve the
accuracy and reliability of the QRS detection algorithm, specifically
in contaminated single lead electrocardiographic data. The algorithm
uses a dual scan of the sample data combined with a peak detection
scheme to locate a reference point on a QRS candidate. The candidate
is then checked for evidence of baseline shift or an excessively low
signal-to-noise ratio. If neither of these criteria is met, the candi-
date is assumed to be a QRS and a fiducial point is located on the
complex.

To assess the sensitivity and specificity of the QRS detection
algorithm, an off-line evaluation was performed on forty-one patient
records collected in the Coronary Care Unit. Arrythmias included in
the evaluation were fast ventricular and atrial rhythms and heart
block. Over 90 percent of the data base was contaminated with exces-
sive muscle artifacts. Of a total of 7,205 beats used in the

evaluation, and positive predictive accuracy were .9641 and .9573, respectively. Of the error, 92.16 percent of the false positives and 84.17 percent of the false negatives were due to excessive noise spike superimposition on the data. None of the false positive error (.0071) was due to P or T wave misidentification as a QRS complex.

These results indicate that a signal-in-noise approach to automated QRS detection is effective in identifying QRS complexes in the contaminated single lead electrocardiogram with minimal error.

TABLE OF CONTENTS

## LIST OF TABLES

LIST OF FIGURES

## ACKNOWLEDGMENTS

My deepest appreciation and respect goes to my friend and mentor, Dr. T. Allan Pryor, for his generous faith and guidance. His spirit will always be an inspiration to me. Also, many thanks to Drs. Frank Yanowitz and Bob Lux for their time and their stimulating ideas. And, finally, a special thanks to my family and friends in Colorado and Utah whose support helped me see the project through to the end.

CHAPTER I

INTRODUCTION

Despite a reversal in the upward mortality trend of ischemic
heart disease beginning in 1963, the disease still causes one-third of
the deaths in the United States annually (Rosenberg and Klebba, 1978).
Of these deaths approximately one-half are due to disorders in cardiac
rate and rhythm (Katz, 1980). The establishment of Coronary Care Units
(CCU) in the early 1960s has been successful in virtually eliminating
primary arrhythmic death in patients with acute myocardial infarction,
largely through the use of continuous electrocardiographic monitoring
in these areas (Lown, Fakhro, Hood, and Thorn, 1967). The acute
coronary care approach, however, has been ineffective in reducing the
incidence of death due to heart failure in these patients. New know-
ledge in the management of acute myocardial infarction patients suggests
that particular arrhythmias occurring in patients suffering from heart
failure can cause further cardiovascular deterioration if not con-
trolled. Improved automated rhythm monitoring can enable earlier
detection and management of these potentially damaging rhythm disorders
in an effort to reduce morbidity in these high risk patients.

Historically, the monitored electrocardiogram provided real-time
and trend data enabling continuous evaluation of management protocols
for the acute myocardial patient in the CCU. The initial goal in the
unit was the immediate resuscitation of patients in cardiac arrest which

became possible with continuous electrocardiographic monitoring. However, Kimball and Killip (1966) reported that this had little effect on overall mortality. It was becoming increasingly evident through electrocardiographic monitoring that patients with acute myocardial infarction had a higher incidence of ventricular arrhythmias which commonly preceded ventricular fibrillation and cardiac asystole, both lethal if left untreated (Spann, Moellering, Haber, and Wheeler, 1964; Julian, Valentine, and Miller, 1964; Day and Averill, 1966). By immediately suppressing these prodromal rhythm disorders with anti-arrhythmic agents, Lown, Vassaux, Hood, Fakhro, Kaplinsky, and Roberge (1967) reported a tenfold reduction in primary cardiac arrest. Thus, early detection of potentially dangerous ventricular rhythm disorders and intervention with antiarrhythmic therapy was effective in reducing the incidence of primary arrhythmic death.

With the development of full-time specially trained emergency teams and earlier detection provided by continuous rhythm monitoring in these units, a substantial improvement in the long-range survival following resuscitation also became evident. Prior to the establishment of CCUs, the percentage of recovery after resuscitation was less than 5 percent (Himmelhoch, Dekker, Gazzaniga, and Like, 1964). Flynn and Fox (1966) reported a long-range recovery of 38 percent of 121 cardiac resuscitations performed in various CCUs. Both the trauma involved in emergency resuscitation procedures and the myocardial deterioration that can result from such an emergency situation stresses the clinical importance of early detection of potentially lethal arrhythmias.

The focus of the modern CCU has been to identify factors which

further compromise the clinical state of the heart failure patient. New knowledge concerning the underlying consequences of particular recurring arrhythmias in the infarcted heart indicate that myocardial tissue necrosis is a dynamic process. Katz (1980) reported that the final infarct size was related not only to the magnitude of the initial insult but also to the cardiovascular events which occur subsequent to infarction. Recurring arrhythmias can further reduce coronary perfusion amidst an increased myocardial need for oxygen, thereby increasing the risk of enlarging the necrotic tissue mass. The extent of infarct has been shown to be a strong determinant of ventricular arrhythmias and mortality (Geltman, Ehsani, Campbell, Schechtman, Roberts, and Sobel, 1979). When more than 50 percent of the left ventricle is damaged, the result is usually lethal (Killip, 1978). Therefore, it is important to promptly manage particular arrhythmias which have been identified as having the potential to increase infarct size.

Power failure rhythms which have been defined as sequalae to heart failure have been reported to enlarge the infarct size if not controlled (Margolis and Wagner, 1976). The more common power failure rhythms include sinus tachycardia, atrial flutter, and fibrillation. Patients having any one of these rhythm disorders have three times the risk of mortality of an individual not exhibiting any of these rhythms. Second degree and complete heart block can also lead to an extension of the infarct or serious tachyarrhythmias if not managed. With complete heart block the escape pacemakers are typically in the bundle branches or Purkinje system and are potentially unreliable. Second degree heart block precedes three-fourths of the cases of

complete heart block and both can invoke irreversible myocardial damage.
Hence, more accurate detection and treatment of these potentially
lethal disorders can improve prognosis in patients suffering from heart
failure.

## The Electrocardiogram

The electrocardiogram (ECG) is a body surface representation of
the electrical events occurring in the heart and is obtained by record-
ing changes in potential between two exploring electrodes (bipolar lead
system) or one exploring and one reference electrode (unipolar lead
system). The electrical activity is caused by dynamic changes in ionic
permeability of the cell membrane. The polarity (negative) of the rest-
ing cell interior is due to the active transport of sodium (Na) ions
out of the cell in exchange for potassium (K) ions by the sodium pump.
Since the resting membrane allows K ions to permeate the membrane but
is impermeable to Na ions, the K ions leak from the inside causing a
build-up of positive charges outside the cell. This results in a rest-
ing membrane potential of -90 mV. As the electronegativity of the
interior decreases to the threshold potential (-75 mV), electrical cur-
rents are generated across the membrane. This process, called
depolarization, is caused by the inward currents which result from the
flow of positive ions, Na and calcium (Ca), into the cell. Once the
membrane potential is reversed to approximately 20 mV, Na and Ca trans-
port channels close and the membrane is again permeable to K ions.
During this phase (effective refractory period) of the action poten-
tial, a depolarizing stimulus cannot initiate a propagated action

potential. With the exchange of Na ions for K ions the sodium pump returns the cell to its normal resting membrane potential. The outward currents generated by the flow of positive ions (K) out of the cell is the process called repolarization. The inward and outward currents are collectively called an action potential.

The initial depolarizing stimulus causes surrounding cell membranes to open Na and Ca channels. In this way a wave of depolarization is propagated through the myocardium. Certain types of cells exhibit automaticity--the ability to automatically depolarize. The mechanism by which cells can generate an electrical impulse is in the inherent impermeability of their resting membrane to K ions. The sodium pump transports K ions to the cell interior where they become trapped, having a neutralizing effect on the polarity of the cell interior.

The normal pacemaker of the heart is the sino-atrial (SA) node located in the upper region of the right atrium. Additional cells exhibiting automaticity are found in the lower atrioventricular (AV) node (40-55 impulses/minute), and the His Purkinje system (25-40 impulses/minute). Since the SA node discharges impulses at the most rapid rate of all of the pacemaker cells (60-100 impulses/minute), it paces the heart. Should the SA node fail, one of the "escape" pacemakers found in the AV node or the His Purkinje system can take over.

## Conduction System

The electrical impulse generated in the SA node sets up a wave of depolarization which spreads through the myocardium by specialized conduction pathways. All myocardial cells have the ability to

propagate impulses but the cells comprising the conduction system have
the ability to conduct impulses at faster rates. The preferred pathways
through the atria are three bands of tissue (internodal tracts) which
are distributed in both the left and right chambers. The internodal
tracts converge on the AV node which connects the atria to the ventri-
cles. The speed of conduction through the nodal cells is slow, around
.02 to .04 meters/second compared to conduction velocities of 1 meter/
second through the atrial myocardium. The delay in propagation of the
impulse through the AV node allows for ventricular filling from the
atria.

Once past the AV node the depolarizing wave conducts through the
AV bundle and down the right and left divisions of the bundle branches
simultaneously. The bundle branches run along the intraventricular
septum to the apex of the heart where each branches into Purkinje fibers
which line the endocardial walls of both ventricles. The Purkinje
network and the Purkinje fibers of the bundle branches are specialized
for very rapid propagation of impulses (.2-.4 meters/second) to the
ventricular myocardium. This insures quick delivery of the depolariz-
ing stimulus to the large ventricular mass so that a cohesive
ventricular contraction can occur. The speed of impulse conduction
through the ventricular myocardium is slower than that in the Purkinje
fibers and atrial myocardium, traveling approximately .3-1.0 meters/
second.

Electrocardiogram Descriptors

Under normal circumstances the first deflection on the ECG

(see Figure 1) is the P wave which represents the depolarization of the atrial myocardium. The time taken for the depolarizing wave to traverse the atria takes approximately 160 to 200 msec. A segment of low level signal during atrial repolarization and AV node and His bundle activation follows atrial depolarization. Because of the small amount of tissue involved, the currents generated are not large enough to pick up a potential difference on the body surface using conventional amplifiers. The PR Interval (onset of P wave to onset of QRS complex) represents the time taken from the onset of atrial depolarization to the onset of ventricular depolarization and has a normal duration of 160 to 200 msec. If the PR Interval exceeds 200 msec, some type of AV block is present.

The QRS complex represents ventricular muscle depolarization. Since the rate of impulse propagation is most rapid through the Purkinje fibers, ventricular activation produces the highest frequency deflection on the ECG. The first downward wave in the ventricular complex is the Q wave; any upward deflection is the R wave and any downward deflection following the R wave is the S wave. With some conduction defects an R' wave (second upward deflection) can exist as well as an S' wave. The duration of the QRS complex is typically less than 100 msec but can last up to 200 msec in complete right or left bundle branch block. The repolarization of ventricular myocardium produces the ST segment and the T wave which are low frequency events as compared to the QRS complex.

Arrhymogenesis

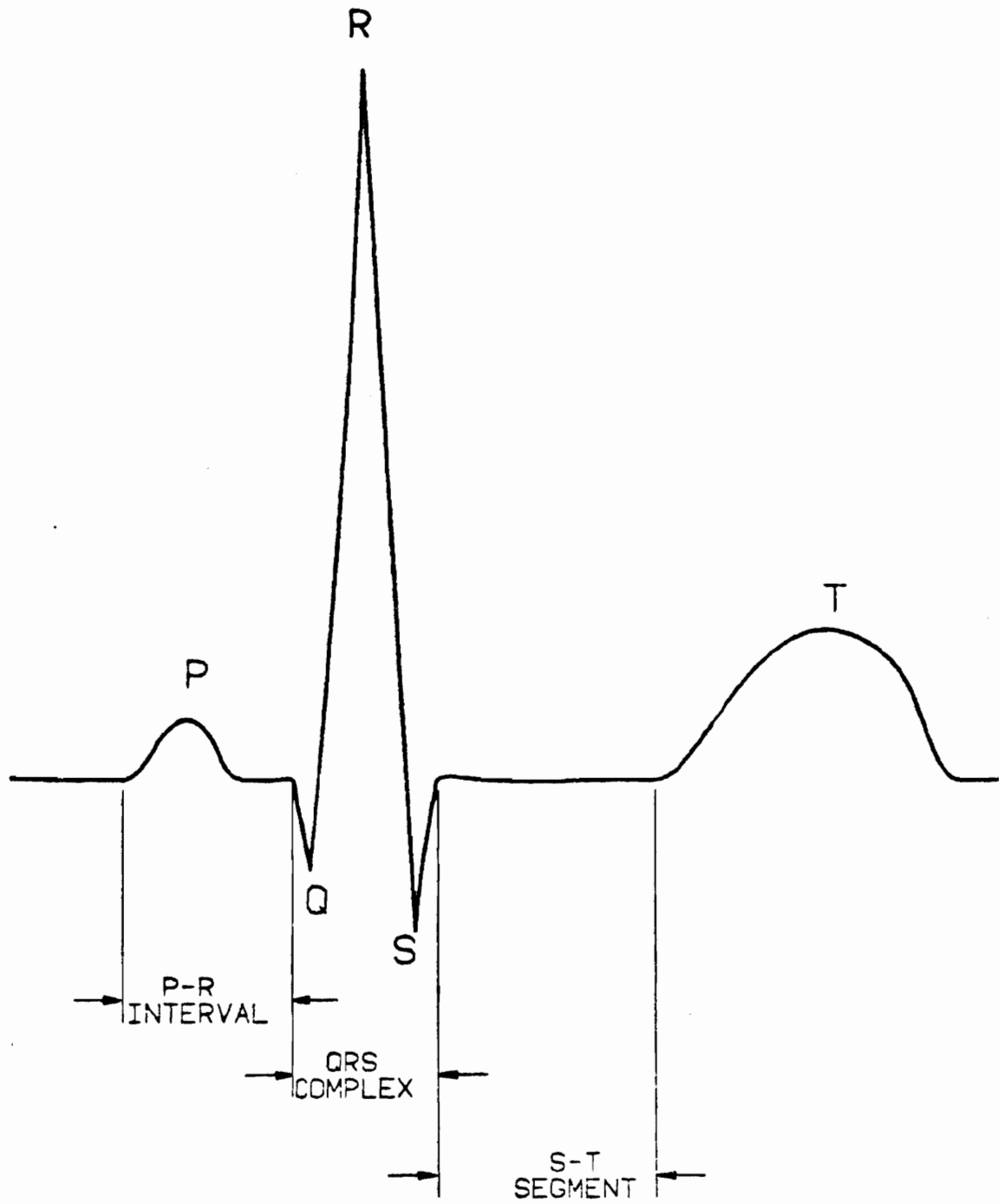Any alteration in cardiac rhythm from normal sinus rhythm

Fig. 1.  Electrical representation of a normal cardiac cycle.

constitutes an arrhythmia and can be attributed to a disturbance in automaticity and/or a disturbance in conduction.

Basically, there are two mechanisms which influence automaticity in normal and/or abnormal hearts. The first mechanism is due to a neuronal or biochemical influence on the normal pacemaker--the SA node--of the heart while the latter results from an ionic imbalance in ischemic regions of the heart. The SA node is innervated by sympathetic and parasympathetic (vagal) nerve fibers which, when stimulated, have an acceleratory or inhibitory effect on the rate of discharge, respectively. An increase in sympathetic tone produces sinus tachycardia (rate > 100 per minute) while excessive vagal influence produces sinus bradycardia (rate < 60 per minute).

Regions of ischemic myocardium can predispose the heart to single or repetitive premature systoles or contractions. An ectopic focus can initiate an impulse if partial depolarization of the cell (to threshold potential) occurs before the normal SA node impulse reaches the cell. In ischemic regions the lack of available oxygen reduces the production of ATP which inhibits the sodium pump. Hence, extracellular K accumulates causing a fall in the resting potential. The acceleration in firing rate of the ectopic pacemaker can initiate a premature contraction, or repetitive premature contractions with sustained firing.

A conduction disturbance is manifested as slowed conduction, loss of the ability to conduct (block, or a process (reentry) which occurs in the presence of both). Slowed conduction can be caused by excessive vagal tone, drugs, or by an impulse entering an ischemic

region. As previously explained, partial depolarization brought on by an ischemic environment partially deactivates the opening of the Na channel causing slowed conduction. In severely affected ischemic regions the membrane potential falls to levels so low that an impulse cannot be initiated or propagated. This causes a block in the conduction of an impulse and can occur in any of the cells of the heart.

Reentry is a process by which an impulse is propagated back to its point of origination. Slowed conduction, coupled with a unidirectional block, allows the impulse to travel around the block and propagate through the blocked region (now capable of reexcitation) in the opposite direction. A unidirectional block can occur in diseased regions of the myocardium where the ability of the cells to propagate an impulse is blocked in one direction. Since repolarization is more rapid in ischemic cells due to the accumulation of extracellular K, the impulse can reenter the localized ischemic area in the opposite direction. Hence, an impulse can give rise to one or more additional impulses by the process of reentry. This phenomenon is believed to be responsible for the sudden onset of the more ominous arrhythmias, namely, atrial fibrillation and flutter and ventricular tachycardia, fibrillation and flutter. Reentrant tachycardias generally occur at higher rates than tachycardias initiated by abnormal impulse formation and represent a more serious threat to cardiac function.

## Historical Perspective of Automated Rhythm Analysis

The clinical importance of early detection of potentially dangerous rhythm disorders was realized by the end of the 1960s.

However, the question of the best approach to detection, i.e., automated or conventional methods, was unsettled. A definitive study by Romhilt, Bloomfield, Chou, and Fowler (1973) demonstrated that conventional monitoring methods were unreliable for the precise and accurate detection of prodromal ventricular arrhythmias. In a retrospective automated analysis of tape recorded electrocardiograms of patients following acute myocardial infarction, prodromal ventricular arrhythmias were detected in virtually all the patients while conventional monitoring recognized these events in less than 20 percent of the patients. They attributed the low incidence of detection by conventional methods to the inability of rate tachometers to respond to transient arrhythmias which did not cause enough change in rate to trigger an alarm. Vetter and Julian (1975) reported similar error results when comparing the detection performance of an analog and computerized alarm system in their Coronary Care Unit. Of the arrhythmias selected as clinically significant for the evaluation, the computer monitor detected 98 percent while the conventional monitoring system detected only 36 percent. Frost, Yanowitz, and Pryor (1977) later reported in an evaluation of the automated arrhythmia alarm system at the LDS Hospital CCU that false positive abnormal alarms occurred only 25 percent as often with the computer system as with the conventional analog system.

Although computerized monitoring has been shown to be the more accurate and reliable approach to arrhythmia detection, cardiac rhythm has proven to be difficult to diagnose with a computer. The performance of real-time automated rhythm monitors is frequented with a considerable number of false and missed alarms despite reported

improved diagnostic accuracy with these systems in the last decade
(Yanowitz, Kinias, Rawling, and Fozzard, 1974; Sanders, Alderman, and
Harrison, 1977; Shah, Arnold, Haberern, Bliss, McClelland, and Clarke,
1977). An evaluation of experimental and commercial real-time rhythm
monitors by Fozzard and Kinias (1976) reports sensitivities for PVC
detection in the range of 78-99 percent (percent total PVCs) with false
positive abnormal rates (percent beats) ranging from .04-.45 percent.
Cox, Nolle, and Arthur (1972) published results of various experimental
rhythm monitor evaluations; sensitivities for abnormal detection ranged
from 67-99.2 percent with false positive abnormal rates (percent
normal beats) in the range of .8-33 percent and false negative rates
(percent abnormal beats) in the range of 0.0-28 percent. The overall
effect of missed and false alarms on the nurses is a lack of confidence
in the monitoring system and a general desensitization to the alarms.
Therefore, further improvement in computerized arrhythmia detection
systems should be directed toward the factors causing the misdiagnosis
of cardiac rhythm.

Among the problems facing automated arrhythmia detection
systems, artifact represents the most serious and frequent source of
error (Pipberger, Dunn, and Berson, 1975; Nolle, 1977; Amazeen,
Moruzzi, and Feldman, 1972). Poor signal condition is caused by fre-
quent muscle artifact induced by patient movement, poor electrode
contact, and electronic pick-up. Engelse and Zeelenberg (1979)
reported a false positive and false negative PVC error of 37 and 24
percent, respectively, using their Automated Arrhythmia Detection
System (AAD). Misclassification of noise accounted for 63 percent of

the false positive PVCs and 53 percent of the false negative PVCs.
In the evaluation of the arrhythmia monitoring system currently in use
at the LDS Hospital CCU, Frost et al. (1977) reported substantial error
due to signal artifact. Forty-seven percent of the alarms generated
during the controlled study were false alarms with artifact the most
common cause of error.

Furthermore, most investigators in this area are in agreement
that the majority of false positives and false negatives can be attri-
buted to errors inherent in QRS detection and delineation schemes
rather than classification per se (Engelse and Zeelenberg, 1979;
Birman, 1982). Mead, Clark, Potter, Moore, and Thomas (1979) reported
that greater than 95 percent of the false positives and 100 percent of
the false negatives can be traced to QRS detection/delineation errors
in the ARGUS/2H system.

In view of the importance of signal artifact in error etiology,
particularly with regard to QRS detection schemes, an examination of the
causes of noise and its manifestations on the ECG follows.

<u>Noise: Definition and Problems</u>

In rhythm monitoring, superimposed noise on the ECG is a com-
mon phenomenon and one of the major obstacles to accurate QRS detection
and delineation. Noise can arise from the electronic devices in the
immediate environment surrounding the patient or from the patient.
The task of distinguishing between noise and ventricular activity
is particularly difficult with the computer because some types
of noise and the QRS share common characteristics, i.e., high

frequency components. These components are used to identify the QRS in the heart cycle. In addition, noise waveforms often correlate highly with the shape of the QRS. In the following sections, physiological and external sources of noise are discussed together with their manifestation on the ECG.

## Sources of Noise

Physiological sources. The physiological sources of noise that can alter the configuration of the ECG are neuronal stimulation and those associated with patient movement. As explained in the last section, the acceleratory and inhibitory effects of sympathetic and vagal stimulation, respectively, cause an increase or decrease in the heart rate. This results in RR interval variation (see Figure 2).

The sources of physiological noise associated with patient movement include changes in the position of the heart in the chest, respiration, and depolarization of nonmyocardial muscle cells. Figure 3 shows an ECG in which the noise is caused by a change in the spatial relationship of the heart in the chest cavity, i.e., a change in the mean QRS vector. This results from the displacement of the heart when the patient changes body positions. The resulting variation in wave amplitude of the QRS, therefore, is not due to factors affecting myocardial contractility, but rather is due to a change in the direction of the mean QRS vector with respect to the stationary, positive recording electrode.

The second source, respiration, causes the chest to move in and out with inhalation and exhalation. This respiratory movement can

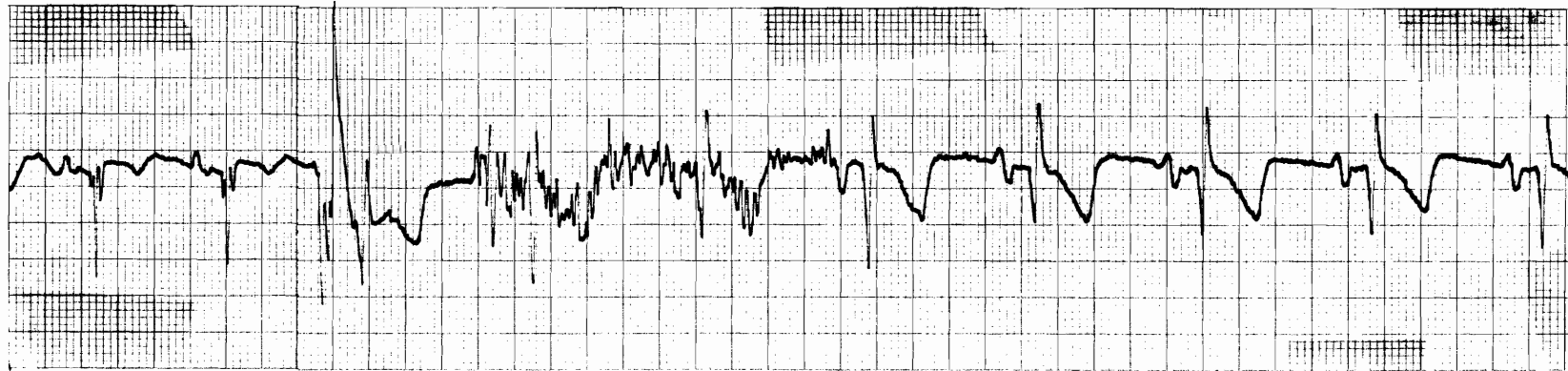Fig. 2.  ECG altered by neuronal stimulation.



Fig. 3.  ECG altered by change in body position.

manifest on the ECG, in the presence of a poor skin electrode inter-
face, as a periodic sinusoidal wave with a frequency equal to the
respiratory rate. Respiratory variation in QRS amplitude can also
result from changes in the volume conductor. Since air is a poor
conductor, an increase in the chest volume with inspiration can re-
duce the signal voltage recorded on the body surface. With expiration
the volume decreases and the amplitude of the QRS can increase.
Figure 4 shows an ECG with manifestations of respiratory variation.

Finally, since myocardial cells are not the only muscle cells
in the body depolarizing, electrical potentials can be generated from
other muscle sources. Electrodes measure the superimposition of all
electrical currents; therefore, potentials generated by skeletal muscle
cells can also be recorded on the body surface. The muscle noise re-
sulting from the depolarization of nonmyocardial cells is randomly
distributed throughout the entire frequency band of the ECG and is one
of the most frequent sources of noise contamination.

Muscle noise can manifest as an abrupt shift in baseline (base-
line shift) and/or a sequence of variable-amplitude noise spikes.
Baseline shifts are caused by sudden patient movement while noise
spikes are the result of muscle cells depolarizing to achieve movement.
An isolated example of baseline shift is shown in Figure 5. A more
common manifestation of patient movement, i.e., baseline shift in
conjunction with noise spikes, is shown in Figure 6, page 17.

External sources. In addition to physiological noise, contamina-
tion of the signal from "external" or electronic noise can occur. The
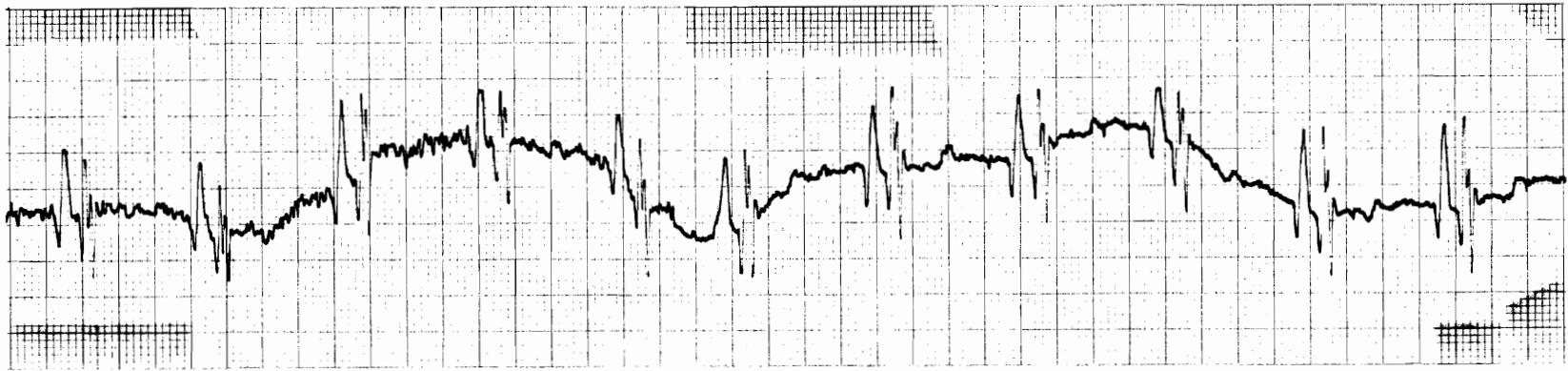barrage of electronic devices powered by sixty cycle alternating

Fig. 4. ECG with respiratory variation.



Fig. 5. ECG with baseline shift.

current in the immediate environment of the patient creates an electrical field which can be sensed by monitoring electrodes. Sixty cycle noise pickup is commonly caused by loose or improperly shielded electrodes. It typically manifests as a 60 Hz sinusoidal wave superimposed on the baseline. Depending on the amplitude of the 60 cycle noise, however, it can manifest as a notch on the QRS complex, P or T wave. Figure 7 shows a rhythm strip contaminated with 60 cycle noise.

Specific electronic devices which are designed to electrically or mechanically stimulate the myocardium also contaminate the electrocardiogram. ECGs of patients with atrial and/or ventricular pacemakers show a high frequency spike before the P wave and/or the QRS complex, respectively, corresponding to the discharge of the electrical impulse. Ventricular pacing spikes are shown in Figure 8.

A less commonly used tool, called a balloon pump, mechanically constricts and dilates the left ventricle. The resulting muscle noise is shown in Figure 9.

## Noise Considerations

All superimposed noise alters the morphology of the electrocardiogram; therefore, its manifestations must, in principle, be taken into account. However, muscle artifact presents particular problems in QRS detection and delineation. This noise can result in high frequency deflections on the ECG and has to be differentiated from ventricular activity. Therefore, the next section reviews various approaches to beat detection in noise contaminated data.
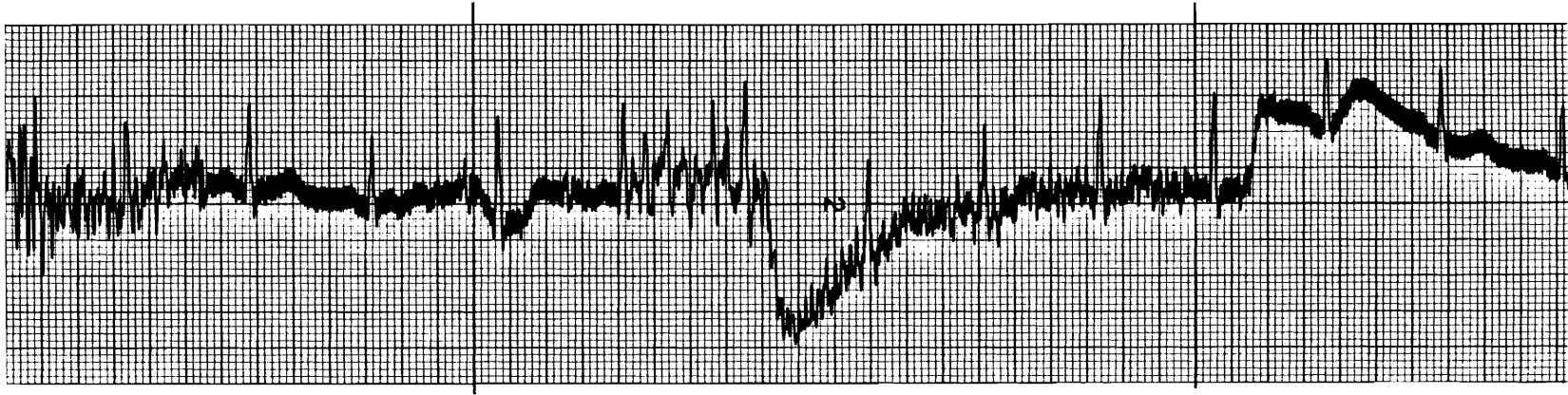
Fig. 6. ECG with random muscle noise contamination.
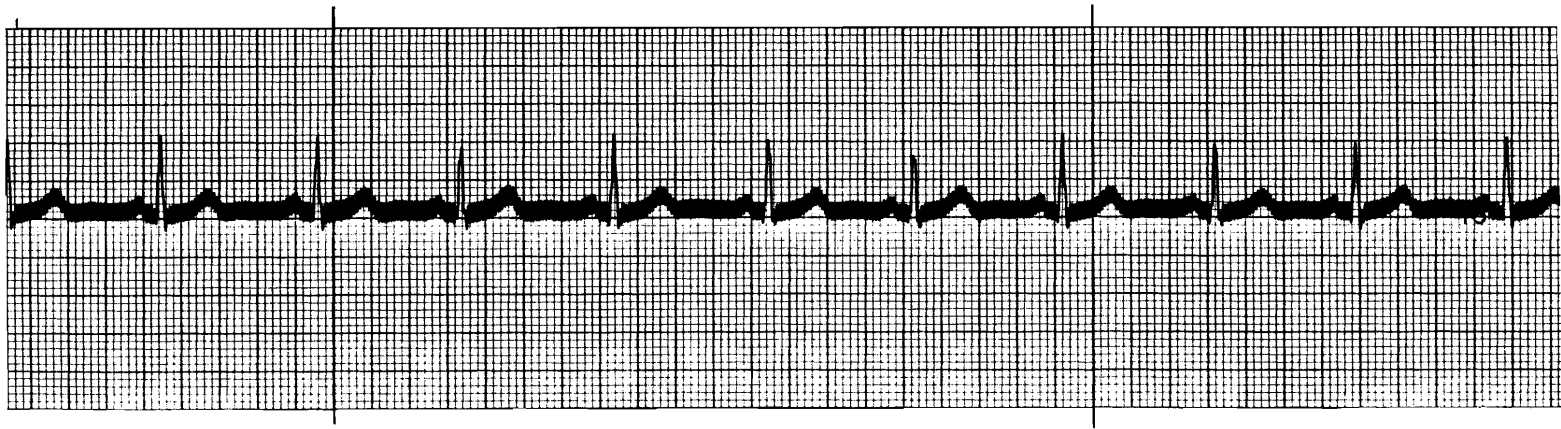


Fig. 7. ECG with sixty cycle noise contamination.

19
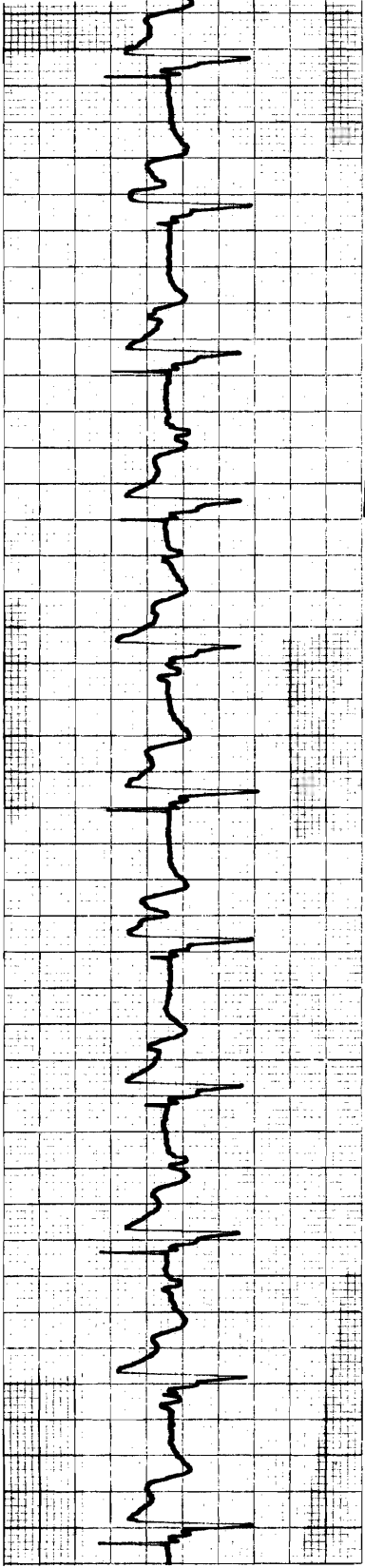
Fig. 8.  Ventricular pacing spikes.
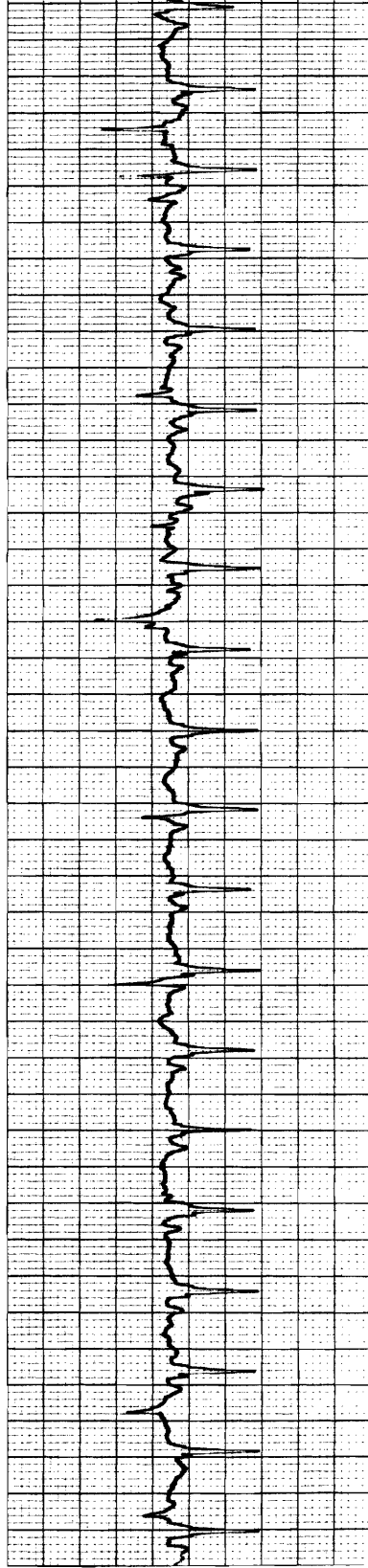


Fig. 9.  ECG distorted by balloon pump.

## Review of Computerized QRS Detection Algorithms

The first reported technique for automatic QRS recognition was
given by Stallmann and Pipberger (1961) in an evaluation of a multiple
lead ECG analysis program used at the Veteran's Administration Hospital
in Washington, D.C.  Single lead arrhythmia detection systems were
developed soon after the first ECG contour analysis programs and used
similar derivative techniques for detection of ventricular activity.
The rate of voltage change is typically expressed by first differences
between consecutive ECG data points.  Since the sampling period is a
constant, the voltage differences are directly proportional to the time
derivatives.  The first difference can be algebraically represented by
the formula:

$$\Delta Y(i) = Y(i+1) - Y(i)$$

where Y(i+1) represents the voltage at the (i+1)th ECG data point and
Y(i) represents the voltage of the ith data point.  The first differ-
ences are computed in a specified time interval at the start of
monitoring; and the maximal positive and/or negative first difference
is assumed to occur on the QRS complex.  Subsequent first differences
exceeding a designated percentage of a maximum first difference is
typically used to flag ventricular activity.

Many variations in the derivative approach have been proposed.
Early investigators used the maximum negative rate of change which
typically occurs on the descending slope of the R-S segment to locate
the QRS (Steinberg, Abraham, and Caceres, 1962).  Hochberg, Weihrer,

McAllister, Calatayud, Zimmerman, and Caceres (1969) at the U.S. Public
Health Service in Washington, D.C. reported in 1969 that QRS detection
in bizarre arrhythmias can best be accomplished using the maximum abso-
lute derivative rather than the most negative.

The percentage of the maximal positive or negative first
difference used is typically dependent upon the number of scans per-
formed to detect a complex.  If a single search is used, the percentage
is typically less than fifty to insure detection of lower frequency
ectopic depolarizations (Geddes and Warner, 1971).  The high false
positive rate resulting from a low tolerance search has prompted some
investigators to use multiple scans (Sanders et al., 1977; Arnold,
Shah, and Clarke, 1975).  Upper tolerances typically exceed 50 percent
of the first difference followed by a lower tolerance search(es), if
necessary.  Multiple scans have been reported to discriminate ventricu-
lar activity more reliably in artifact than single scans.

Other attempts to desensitize the derivative technique to noise
have been reported.  Frankel, Rothmeier, James, and Quaunor (1975)
designate the tolerance as one-eighth the absolute maximum negative
first derivative calculated between two samples 16 msec apart.  A QRS
is detected when seven consecutive points fall below this tolerance.
These investigators found this algorithm to be effective in filtering
out 60 Hz noise.  Haywood, Murphy, Harvey, and Saltzberg (1970) use the
secant rather than the slope for R wave detection, where the secant is
defined by the formula:

$$V'(i) = V(i+4) - V(i)$$

with V (i) the ith data point.  A trigger level (R) is then defined
as:


$$R = V'(min) + 1/6 \; [V'(max) - V'(min)]$$


where V'(max) and V'(min) denote the maximal positive and maximal nega-
tive secants, respectively.  Each time this level is exceeded, the first
minimum derivative falling below this level is considered a reference
point and the beginning of a new cycle.  Reference points typically
fall on the descending limb of the R wave but can occur on the S wave
depending on the lead selected.  The R location was reported to be
consistent in 60 Hz noise.  Knoebel, Rasmussen, Lovelace, and Anderson
(1975) at the Indiana University Medical Center also calculate the
secant (Z') using a four sample displacement and then determine
the mean maximal negative secant and the standard deviation of the
samples (Z'(s)) for ten successive 2.5 second buffers.  The threshold
(T(h)) is then computed as:


$$T(h) = Z' - Z'(s).$$


Knoebel et al. (1975) determined experimentally that a displacement of
four samples provided the most reliable results in excessive muscle
noise.  Another approach proposed by Holsinger, Kempner, and Miller
(1971) at the National Institute of Health at Bethesda, Maryland, is
to designate a percentage of the maximum negative derivative based on
the requirement that a maximum of three consecutive first differences

fall below this tolerance. The tolerance is then continuously adjusted by requiring that a minimum of three but less than seven consecutive differences satisfy the tolerance criteria.

Various digital filters designed for data smoothing have been incorporated in rhythm monitoring systems to further desensitize detection algorithms to signal artifact. Pryor (1971) used a weighted convolution equation:

$$Y(i) = sum (A(k) * X(j-k))$$

where the A(k)s are the weights and Y(i) the output to the digitally filtered signal. This technique causes a minimum of signal distortion and effectively suppresses superimposed noise. Balda, Diller, Deardorff, Doue, and Hsieh (1977) with the HP Medical Products Group use an adaptive filter if the critical points (maxima, minima, and zero crossings) in the ECG record do not fall in the acceptability range. Analysis of the data resumes after filtering.

One of the most widely respected computer programs for monitoring of cardiac rhythms, ARGUS, originally developed by Nolle (1972) as a doctoral project at Washington University, uses a data compression scheme (AZTEC) and QRS detection/delineation scheme (PRIMITIVE) to identify QRS complexes. The preprocessing scheme codes line segments as a slope and a duration. A QRS is detected when a series of line segments satisfy specified sign and number restrictions. ARGUS, however, has been reported to be highly vulnerable to signal artifact (Nolle, 1977; Zeelenberg, Deutsch, Engelse, and Corbeij, 1977). AZTEC

data is screened for characteristic signs such as low data compression or an excessive number of local extrema to identify artifact. PRIMITIVE then requires that AZTEC data be free of detected artifact for at least 800 msec. Sanders et al. (1977) version of ARGUS developed at Stanford University stops all beat detection and delineation upon detected artifact and requires five continuous seconds of nonnoisy data to resume analysis.

Most of the prominent researchers in this field are in agreement that contextual analysis of the electrocardiogram, i.e., analysis of only noise-free data, is not a good solution to the noise problem in the clinical environment (Pipberger et al., 1975; Amazeen et al., 1972; Feldman, 1977). Reported data loss figures due to rejection of noise segments of the ECG have been high (Nolle, 1977; Zeelenberg et al., 1977). Many of the existing rhythm monitoring systems, however, use a contextual approach to analysis because of the lack of better QRS detection and noise detection algorithms.

With this in mind a project was designed to develop signal-in-noise detection criteria which could accurately detect QRS complexes (normal and abnormal) in the contaminated ECG waveform. The conclusions arrived at by investigators in this field are consistent with our findings using the automated rhythm-monitoring system at the LDS Hospital CCU: The majority of false positive (abnormal) alarms are caused by misidentification of ventricular activity. Hence, the objective of this project is to reduce the incidence of false positive complexes detected, while minimizing the incidence of false negatives.

To accomplish this objective, the number of diagnostic criteria

have been increased in the program in an effort to diminish the number of false alarms. An inherent danger in this approach is a rise in the incidence of false negatives which clinically poses a more serious problem than false alarms. Hence, particular emphasis is placed on improving the sensitivity or the ability of the detection criteria to identify true ventricular activity without loss of specificity or ability to distinguish nonventricular activity from true ventricular activity.

The approach to achieve this objective was to gather electro-cardiographic data which was heavily contaminated with noise and representative of a broad spectrum of rhythm disorders, particularly the prodromal and lethal arrhythmias previously discussed. By doing so, development of the QRS detection/delineation criteria could be done on a data base representative of on-line monitored electro-cardiographic data rather than on a simulated or well defined data base.

The first step was to design an inclusive candidate detection algorithm which would flag all possible beats. The candidate set would then be subject to passage of discriminative criteria aimed at identifying noise configurations and assessing levels of muscle artifact. To accurately detect beats using this signal-in-noise approach, the following techniques were pursued. Levels of muscle artifact were determined relative to the amplitude of the QRS com-plex. By rejecting only candidates with low signal-to-noise ratios, the data loss can be minimized. Another approach is to identify specific noise configurations that can be used to distinguish noise

from ventricular activity.  Upon validation of a candidate as a beat by satisfying the above criteria, the final step would be to locate a consistent fiducial point on each complex.

CHAPTER II

METHODS

## Data Acquisition

The lead chosen for rhythm monitoring in the LDS Hospital
Coronary Care Unit is the Modified V1.  Typically, the lead systems
employed for rhythm monitoring are those which best document atrial
activity since the P wave configuration and its relationship to ventri-
cular activation is essential for adequate rhythm analysis.  In
addition, the Modified V1 differentiates between a right and left
bundle branch block, both prodromal post-MI conduction disorders.
For these reasons, the Modified V1 is the lead of choice for rhythm
monitoring in this coronary care unit.

The amplified ECG can be accessed from any of the twelve beds,
including the four acute beds, from the Central Monitoring Station in
the unit.  The analog data were recorded with a four channel Hewlett-
Packard tape recorder onto magnetic instrumentation recording tape at
3 3/4 ips.  The data were then digitized on a Data General NOVA 3
computer equipped with a 10 bit A/D converter at a sampling rate of
200 sps.  For long-term storage the samples are written to an indexed
data file on floppy disc using a double-buffering technique.  When
needed for algorithm development, a data file is transferred to the
hard disc on the ECLIPSE computer.

The amount of continuous data recorded for the off-line

analysis of each patient data file is limited by the inherent addressing capabilities of the developmental computer--a Data General ECLIPSE S200. The extent of memory which can be directly accessed has an upper addressable limit of 32,767, 16 bit words. This is approximately 164 seconds (2 minutes, 44 seconds) of data. The American Heart Association recommends 30 seconds to 1 minute rhythm strips for accurate interpretation of rhythm disturbances. Approximately 5 minutes of data were recorded on each rhythm, with the excess providing a backup to the initial 32K samples.

The decision to sample at 200 sps was based on practical and theoretical considerations. A common practice in signal analysis is to sample at twice the highest frequency component in the signal to prevent aliasing (based on the Nyquist theory). The American Heart Association recommends that all recording equipment used in the monitoring of the ECG have a flat frequency response out to 100 cps. Therefore, similar detail is present in the analog recording as the digital data sampled at 200 sps.

## QRS Detection Algorithm

The initial task in the detection of a QRS complex is the initialization of the beat detector. Since the QRS represents the highest frequency "waveform" in the noise-free heart cycle, differences between consecutive samples will be a maximum during the QRS. This maximum first difference must be calculated as well as the complex search region. Therefore, to initialize the beat detector, the following steps are necessary:

1.  Find the maximum absolute first difference (MXDF) in the initial 3 seconds, i.e., MXDF = max (abs (X(i) - X(i+1)))
i = 0 to 599 where X(i) is the A/D value of the ith sample in the sample data array X.

MXDF is typically found in the region of most rapid impulse conduction, i.e., the bundle branch system of the ventricles (.4 meters/ second). This 3 second region must not include high frequency noise or exclusively ventricular tachycardia, flutter, or fibrillation since either of these conditions could cause misdetection of subsequent complexes.

2.  Set the first- and second-pass candidate tolerances, CTOLR60 and CTOLR16, equal to 60 and 16 percent, respectively, of MXDF:  CTOLR60 = (.60 * MXDF); CTOLR16 = (.16 * MXDF).

3.  Set the first- and second-pass boundary tolerances, BTOLR16 and BTOLR30, equal to 16 and 30 percent, respectively, of MXDF:  BTOLR16 = (.16 * MXDF); BTOLR30 = (.30 * MXDF).

4.  Limit the complex search region (CPLX-REG) to the number of samples corresponding to two-thirds of twice the mean RR Interval over the initial ten complexes:  CPLX-REG = 1.32 * ((sum (RRARRY(i)) / (i-1)) i = 2 to 10, where RRARRY(i) is the RR Interval of the ith beat in the RR Interval array RRARRY.

Once the tolerances and complex search region are initialized, the sample data is scanned in order to identify a QRS complex region (candidate) using a derivative technique. To localize a complex region, the following steps are necessary:

1.  Set the beginning of the candidate search region

(CAND-REG1) equal to 3 seconds relative to the beginning of the
sample data file.  Set the end of the candidate search region
(CAND-REG2) equal to the beginning of the candidate search region
plus the complex search region:  CAND-REG2 = CAND-REG1 + CPLX-REG.

2.  Beginning with the CAND-REG1 calculate consecutive first
differences:  fdiff = X(i) - X(i+1) i = CAND-REG1 to CAND-REG2.
If the fdiff exceeds CTOLR60, then i is labeled the candidate's
time of occurrence relative to the beginning of the sample data
file.

3.  If a candidate is not located in the first-pass of the
complex search region, then implement a second-pass search using
CTOLR16 as the critical candidate tolerance.

4.  If a candidate is not located in the second-pass of the
complex region, the candidate search region is incremented:
CAND-REG1 = CAND-REG2; CAND-REG2 = CAND-REG1 + CPLX-REG.
The dual tolerance approach to QRS complex recognition, i.e., lack of
a qualifying first difference on an initial high tolerance search
necessitating a second lower tolerance search, is needed in a multi-
focal complex environment.  That is, changes in complex morphology that
are initiated by abnormal impulse formation below the AV node (and not
blocks which use the bundle branch system) necessitate a second search
for complex detection.  This is because ectopic ventricular depolariza-
tions use a less efficient conduction system, the venticular
myocardium.  Therefore, first differences are typically less than
differences in complexes initiated from an atrial focus.

Once a complex region is flagged, a "dominant" peak is located

in the next 150 msec (PK-REG). The peak detector identifies the most
highly correlated interval of samples to a 100 msec duration peak.
The filter is designed to detect a peak morphology using the follow-
ing weights: (-1,0,0,0,0,0,0,0,0,2,0,0,0,0,0,0,0,0,-1). The weighted
convolution equation:

$$Y(i) = \text{sum } (H(j) * X(i-j)) \quad j = -n \text{ to } n$$

where X(i) is the A/D value of the ith sample in the sample data array
X, H(j) the weight as a function of the interval value j, n the
interval, and Y(i) the output to the equation reduces to the equation:

$$Y(i) = \text{abs } (2 * X(i) - X(i-10) - X(i+10))$$

using a 10 sample interval. When the output Y(i) is at an absolute
maximum, i is labeled the peak's time of occurrence (PK-TOC) relative
to the beginning the sample data file. The PK-TOC is designated the
candidate's fiducial point and is used as a reference for obtaining
features which are necessary to validate the candidate as a QRS
complex.

This set of features stored for each candidate is used to
validate each subsequent candidate once an initial beat is validated.
Among these features are the RR Interval, the prepeak interval ampli-
tude and the postpeak interval amplitude. The candidate RR Interval
(RR) is defined as the number of samples between the current PK-TOC
and the last validated peak's time of occurrence (LST-PK-TOC):

$$RR = PK\text{-}TOC - LST\text{-}PK\text{-}TOC.$$

The RR is assigned to the previous candidate RR Interval (LST-RR) after each new complex is validated. The prepeak and postpeak interval amplitudes (PREPK-AMP and POSTPK-AMP) represent amplitude offsets referenced to the candidate peak. Each value represents the change in amplitude between two nonconsecutive samples (toc1 and toc2) where toc1 and toc2 are the PK-TOC and a designated interval limit, respectively. The interval limit is equal to twelve samples; therefore, the PREPK-AMP and POSTPK-AMP represent -/+ 60 msec offsets, respectively, about the PK-TOC and can be expressed as:

$$PREPK\text{-}AMP = X(PK\text{-}TOC) - X(PK\text{-}TOC - 12)$$

$$POSTPK\text{-}AMP = X(PK\text{-}TOC) - X(PK\text{-}TOC + 12).$$

Before the boundary values (QRS onset and offset) are located, the following conditions must be met:

1. The complex must pass the noise criteria (defined in the next section).

2. The instantaneous heart rate must be less than 200 beats per minute, i.e., RR > = 300 msec.

If both conditions are true, the candidate is accepted as a valid QRS complex. If the candidate violates the initial condition, the candidate is rejected as noise. If the second condition is met, the following exception to boundary location is required if the LST-RR

also corresponds to a heart rate greater than 199 bpm:

1.  No boundary search (defined below) occurs and the PK-TOC is used as the fiducial point (onset) and the "offset" of the complex.

2.  A polarity check is required.

The polarity algorithm requires that the prepeak interval amplitudes of the current and previous candidate (PREPK-AMP and LST-PREPK-AMP) have the same sign.  This check is necessary to insure consistent fiducial point location in rhythms exhibiting rates in excess of 199 bpm.  Since it is reasonable to assume that tachycardia morphologies exceeding 199 bpm, i.e., typically ventricular flutter and fibrillation, are commonly represented as alternating peak polarities in sequence, it is required that consecutive fiducial points be located on similar peak polarities.  Using this polarity requirement, misclassification of similar beat morphologies is minimized.  In addition, the RR Interval more accurately represents the actual timing between beats.

The QRS delineation scheme locates an onset and offset on the complex.  The QRS onset represents the fiducial point of the complex while the "offset" provides a consistent reference point to which the skip region is added once a beat has been detected.  The location of an "offset" does not necessarily reflect the actual completion of ventricular depolarization (J point), i.e., can be the onset of the T wave, T wave peak, etc.  The overriding consideration is that the offset location be morphologically consistent on similar complexes.

A derivative technique similar to that implemented for

candidate location is used for boundary location. The following steps are necessary:

1. Designate the beginning of the onset, offset search regions (ONST-REG1, OFST-REG1) as -/+ 30 msec about the PK-TOC, respectively: ONST-REG1 = (PK-TOC - 6); OFST-REG1 = (PK-TOC + 6). Designate the end of the onset, offset search regions (ONST-REG2, OFST-REG2) as -/+ 150 msec about the PK-TOC, respectively; ONST-REG2 = (PK-TOC - 30); OFST-REG2 = (PK-TOC + 30).

2. Beginning with ONST-REG1 search backward 120 msec for three consecutive absolute first differences less than BTOLR16 to locate the onset. If a sample interval satisfies this condition in the onset search region, then the onset is labeled the time of occurrence of the initial sample in the interval (ONST-TOC). Likewise, search forward 120 msec beginning with OFST-REG1 for six consecutive absolute first differences less than BTOLR16 to locate the offset. If an interval satisfies this condition in the offset search region, then the offset is labeled the time of occurrence of the initial sample in the interval (OFST-TOC).

3. If an interval of four or seven samples (depending on type search) does not satisfy the previous requirement, then implement a second-pass absolute first difference search in each respective region using BTOLR30 as the critical boundary tolerance. This second search is necessary for onset and/or offset location when high frequency noise is superimposed on either region.

4. If an interval of samples in the onset search region does not satisfy the above requirement using a second search, then the candidate is rejected as being too noisy. If the offset criteria is not satisfied, then the offset's time of occurrence is assigned 30 msec following the PK-TOC: OFST-TOC = (PK-TOC + 6).

Once a fiducial point has been located on the beat, the RR Interval (RR-INTV) is calculated:

$$RR\text{-}INTV = ONST\text{-}TOC - LST\text{-}ONST\text{-}TOC$$

where the LST-ONST-TOC corresponds to the last validated beat's onset time of occurrence. The (onset) RR-INTV more accurately represents the actual timing between validated beats than the candidate RR Interval (RR) since onset location is more consistent than peak location on similar beats (discussed in Results). Therefore, all rate dependent calculations employed in a classification scheme should use the more accurate interval, RR-INTV.

Once the RR Interval has been calculated, one of four no-search regions is designated based on the instantaneous heart rate. If the heart rate is:

1. Greater than or equal to 300 bpm, then skip forward 50 msec from the PK-TOC

2. Less than 300 bpm but greater than or equal to 200 bpm, then skip forward 150 msec from the PK-TOC

3. Less than 200 bpm but greater than 120 bpm, then skip

forward 150 msec from the OFST-TOC

4. Less than or equal to 120 bpm, then skip forward 250

msec from the OFST-TOC.

The first-pass candidate search resumes with the initial sample fol-

lowing a no-search region.

## Noise Detection Algorithm

As previously stated, muscle artifact contributes the majority

of false positive error in candidate location due to the high fre-

quency components superimposed on the waveform.  Two manifestations

of muscle artifact superimposition, which are identified in the noise

detection algorithm, are baseline shifts and high frequency noise

spikes.

## Baseline Shift Identification

To identify a candidate as a shift in baseline due to non-

myocardial potential superimposition, the peak morphology is checked

for evidence of "one-leggedness."  As defined in the previous sec-

tion, two legs, the PREPK-AMP and POSTPK-AMP, are calculated for each

candidate peak.  When a baseline excursion occurs due to patient move-

ment, a large disparity in these magnitudes results.  Using the

absolute value of each leg:


$$LEG1 = abs (PREKP-AMP)$$


$$LEG2 = abs (POSTPK-AMP),$$

the ratio of minimum to maximum leg is calculated: LEG-RTO = min (LEG1,LEG2) / max (LEG1,LEG2). If the magnitude of the minimum leg is less than 25 percent of the maximum leg (i.e., LEG-RTO < .25), then the candidate is labeled a shift in baseline and rejected as noise.

## Nonpeak Identification

Taking into account the morphology of a peak, i.e., two ascending intervals (maximum) or two descending intervals (minimum) about a peak, a nonpeak is identified when the prepeak and postpeak interval values, PREPK-AMP and POSTPK-AMP, exhibit dissimilar sign. Candidates labeled as nonpeaks are rejected as noise.

## Noise-Spike Identification
## and Quantization

To assess the "level" of noise spike superimposition about a peak, maxima and minima that meet signal to noise (S/N) requirements are counted. To locate and verify an extremum, the following steps are required:

1. Set the signal S(i) equal to the output of the peak detector: S(i) = abs (2 * X(i) - X(i-10) - X(i+10)), where i corresponds to the PK-TOC of the candidate.

2. Set the noise tolerance, NTOLR15, equal to 15 percent of S(i): NTOLR15 = (.15 * S(i)). If NTOLR15 is less than or equal to 10 A/D units (corresponding to S(i) < 66), then output the message "Increment the Gain" and default NTOLR15 to 1. Unless the gain is incremented, the probability of detection error is increased due to the low signal to noise ratio.

3. Designate the beginning, end of the maxima/minima search region (MXMN-REG1, MXMN-REG2) as -/+ 150 msec about the PK-TOC, respectively: MXMN-REG1 = (PK-TOC - 30); MXMN-REG2 = (PK-TOC + 30).

4. Beginning with MXMN-REG1 calculate consecutive first differences: fdiff1 = X(i); fdiff2 = X(i+1) - X(i+2). If fdiff1 and fdiff 2 exhibit opposite sign, designate the extremum as a maximum or minimum time of occurrence depending on the sign order: MX-TOC = [(-)fdiff1, (+)fdiff2]; MN-TOC = [(+)fdiff1, (-)fdiff2]. (NOTE: These sign assumptions are based on unsigned A/D values with the maximum A/D value representing maximum voltage, the minimum A/D value representing minimum voltage).

5. To qualify the maximum or minimum as a valid noise candidate (N(i)), the following steps are necessary:

a. Set amplitude limits of the potential maximum, minimum equal to -/+ NTOLR15 about MX-TOC and MN-TOC, respectively: MAX-LMT = (MX-TOC - NTOLR15); MIN-LMT = (MN-TOC + NTOLR15).

b. To verify a potential maximum, continue an incremental first difference calculation beginning with MX-TOC: fdiff = X(i) - X(i+1) where the initial value of i is MX-TOC. Validation of the maximum occurs when the following conditions are true: (1) X(i+1) < MAX-LMT and (2) inclusive first difference sign(s), i.e., in region beginning with MX-TOC and ending with sample i satisfying the initial condition, are

positive. To verify a potential minimum, continue an incremental first difference calculation beginning with MN-TOC: fdiff = X(i) - X(i+1) where the initial value of i is MN-TOC. Validation of the minimum occurs when the following conditions are true: (1) X(i+1) > MIN-LMT and (2) inclusive first difference sign(s), i.e., in region beginning with MN-TOC and ending with sample i satisfying the initial condition, are negative. If condition 2 is violated before condition 1 is true, the extremum is invalidated.

    c. Upon validation, MX-TOC or MN-TOC is stored in N(k). If k is greater than 7 (i.e., > 7 extrema corresponding to an S/N ratio < 6.67), then the candidate is rejected as being too noisy.

CHAPTER III

JUSTIFICATION OF METHODS

## Approach

To design a robust QRS detection delineation algorithm, the following phases were implemented:

1.  Visual identification of all complexes in each data file

2.  Refinement of the algorithm to achieve minimum QRS detection error in the data base.

An overview of the data is listed in Table 1. Of the forty-one data files, fifteen rhythm disturbances are represented (excluding normal sinus rhythm). Note that the prodromal and lethal arrhythmias discussed in the first chapter are included in the data set. In addition, high frequency noise is superimposed on more than 90 percent of the patient data files.

The initial phase involved generating a validated index file (for each patient data file) containing feature specific time of occurrences located by the candidate detection algorithm. Features included in each validated file were peak, onset and offset time of occurrences, respectively. To verify accurate detection of the complex, a patient data file was transferred to memory from the disc, the algorithm executed, and then the respective features located were superimposed on the waveform and verified using a Tektronic graphics terminal. In order to validate a peak time of

TABLE 1

DATA BASE OVERVIEW

| Rhythm | Number of Data Files | Total Seconds |
|---|---|---|
| NSR | 3 | 404 |
| NSR with PACs | 1 | 128 |
| NSR with PVCs | 11 | 1,423 |
| NSR with PACs and PVCs | 1 | 163 |
| NSR with PVCs and Paced | 1 | 163 |
| NSR with PSVT | 1 | 46 |
| Atrial Fibrillation-Flutter | 1 | 40 |
| Atrial Fibrillation with PVCs | 4 | 440 |
| PSVT | 2 | 245 |
| PSVT with PVCs | 3 | 491 |
| PSVT with AV Block | 1 | 76 |
| AV Block | 2 | 322 |
| Bundle Branch Block | 3 | 394 |
| Accelerated Ventricular Rhythm | 2 | 220 |
| NSR with Ventricular Tachycardia | 2 | 245 |
| NSR with Ventricular Fibrillation-Flutter | 3 | 87 |
| Total | 41 | 4,894 |

NOTE:  NSR = normal sinus rhythm; PAC = premature atrial depolarization; PVC = premature ventricular depolarization; PSVT = paroxysmal supraventricular tachycardia; and AV = atrio-ventricular.

occurrence, the location had to be accurate (i.e., the apex of the most prominent peak in the QRS) and consistent (i.e., the same location on each complex). If a complex was not detected, the criteria were modified in an effort to isolate the appropriate peak time of occurrence. After a valid peak time of occurrence was identified for all complexes, including those contaminated with noise, the time-specific values were stored in a validated index file (filename.VIDX) and stored on the disc.

Considerable variation in the empirical values was necessary to arrive at a complete set of peak time of occurrences for each file. Not only was there variation among complexes in a file but variation from file to file.

The second phase involved converging on a fixed set of parameter values that represented minimal error in complex detection and delineation over all the data. First, it was necessary to isolate the best combination of values for each file. To achieve this, a value-specific index file was generated using the same algorithms that produced the validated index file. By comparing this file to the validated index file, the error (FN and FP) between the two files could be quantitated. The goal was to converge on a minimum error combination of values.

The initial approach to identifying the minimum error combination was to input n values (n = 1,10) for each of the nine parameters. Each value-specific file generated was then compared to the validated index file and the error calculated. In theory, the ten combinations of values with minimum error generation were to be saved. Practically,

the cycle time (execution of one combination/one record) was approximately 25 msec, therefore, requiring approximately twenty-four years to execute one billion combinations for a thirty-two record file. Even to execute a five value minimum error evaluation (thirty-two records) would take approximately seventeen days. Therefore, it was necessary to change from a multivalue to a single value approach.

Using the experience gained from the validated index file generation, a good guess at the "best" combination of values was possible. This approach, coupled with the justification of all FN and FP errors, ultimately defined all parameter values. The error justification identified all worst-case phenomena, thereby reducing the number of false negatives.

## Justification of QRS Detection Criteria

### Dual Complex Search

The use of a dual complex search is necessary to meet the peak search region (PK-REG) and complex tolerance constraints. The PK-REG is limited by the minimum RR Interval since it should not include more than one complex. This occurs between consecutive flutter beats and is thirty points (corresponding to a rate of 400 bpm). Therefore, to prevent nondetection of a flutter beat, the PK-REG is set equal to thirty samples.

The complex tolerance must be small enough to flag PVCs. To quantitate the percent of the maximum absolute difference necessary to detect all PVCs, noise-free PVCs were searched thirty points prior to the peak time of occurrence (PK-TOC). The maximum difference

between consecutive points in this region represents a percentage of
the maximum difference calculated in the first 600 points (MXDF).
Figure 10 shows a histogram with the relative frequencies of maximum
percent (for each PVC) of MXDF. Only maximum percentages less than
40 percent MXDF are plotted. Of the 250 PVCs searched, the minimum
percent of MXDF was sixteen, with 14.8 percent of the PVCs less than
30 percent of MXDF, 29.6 percent of the PVCs between 30-40 percent
MXDF, and 55.6 percent of the PVCs exceeding 40 percent MXDF. The
minimum percent of MXDF was shared by two PVCs, one isolated occur-
rence and the other in a ventricular tachycardia sequence.

With the tolerance set equal to 16 percent of MXDF, the P wave
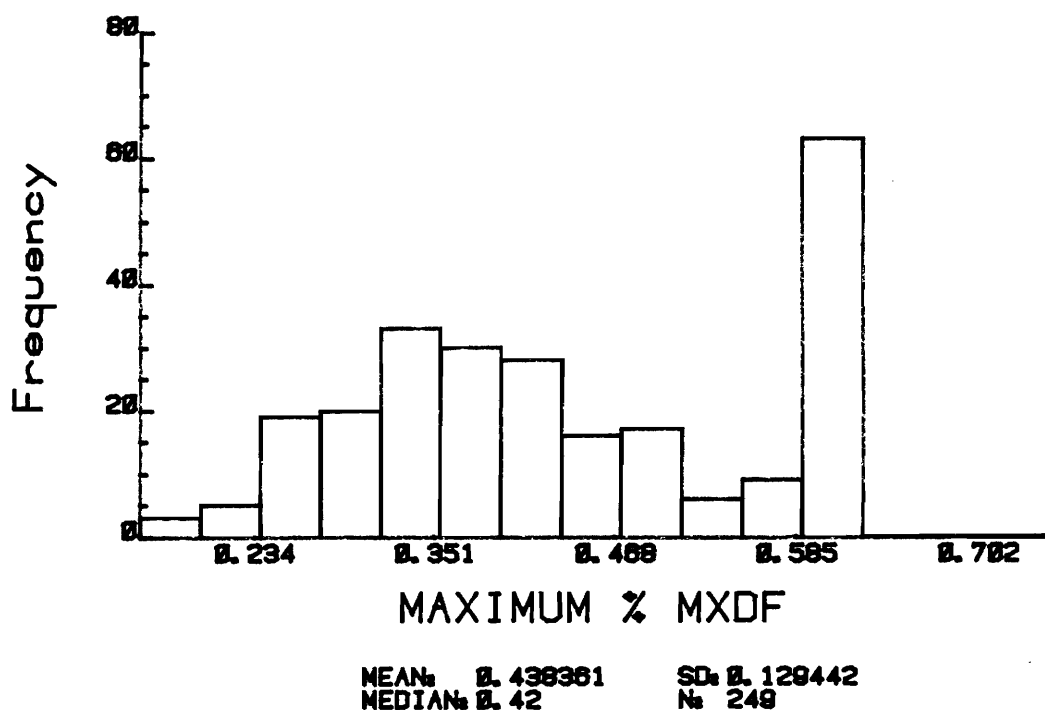would be flagged in the normal heart cycle. Since the normal range



Fig. 10. Frequency of maximum percent of PVCs first differ-
ences.

for the PR Interval is 120-200 msec (twenty-four to forty points),
the PK-REG could fall short of the QRS complex thereby detecting the
P wave.  In addition, some arrhythmias such as AV block have prolonged
PR Intervals insuring P wave detection.  Therefore, it is necessary
to use a first search to detect the majority of complexes and a
second, lower tolerance search to detect lower frequency complexes.

The success of a dual complex search depends on the designa-
tion of an appropriate complex search region (CPLX-REG).  The CPLX-REG
must be limited to one complex since second-search phenomena (i.e.,
PVCs) might not be detected if more than one complex is included.  With
the majority of PVCs compensatory, one and one-third average RR
Intervals would include the PVC but not the following beat.  Some
error has been attributed to this search region, however, and is dis-
cussed in the next chapter.

## Peak Polarity Check

The polarity check insures that consecutive tachycardiac and
flutter complexes are detected consistently.  Rhythms with rates
equally or exceeding the minimum tachycardia rate (200 bpm) include
supraventricular and ventricular tachycardia (150-250 per minute) and
ventricular flutter and fibrillation (200-300 per minute).  Because of
the sinusoidal configuration of some tachycardic (typically exceeding
199 bpm) and flutter waves, the location of the PK-TOC on the wave
varied from the peak R wave to the peak T wave.  The importance of
locating similar morphological complexes in a consistent location is
to prevent labelling similar beats as different morphologies.

Rejection based on different peak polarities, however, can cause a missed beat. Sequences of ventricular beats (i.e., idioventricular rhythm or ventricular tachycardia) ending in a fusion beat or returning to normal sinus rhythm can cause rejection of the initial takeover beat if the minimum tachycardia rate is less than the ventricular rate. Rejection of some multifocal complexes in a run of ventricular tachycardia can also occur if the minimum tachycardia rate is sufficiently low. Because of the potential rejection of valid complexes associated with fast ventricular rhythms and "slower" ventricular tachycardias (i.e., rate between 100-200 bpm), the minimum tachycardia rate was set equal to 200 per minute. Therefore, ventricular rhythms whose rates exceed 199 bpm and ventricular flutter and fibrillation waves are subject to a peak polarity check.

## Onset, Offset

The designation of the QRS onset and offset is necessary to define complexes and the skip region between them, respectively. The QRS onset provides a consistent fiducial point for the complex. Attempts to use peaks (PK-TOC, local peak time of occurrences) or mean area as the fiducial point failed because of the inherent inconsistency in location. The location of the QRS offset is necessary to define skip regions between complexes. The original skip region added to the PK-TOC was limited to thirty points to prevent skipping over a flutter wave in succession. Using this algorithm, however, caused ventricular complexes with T wave inversion to be detected twice on the same complex (i.e., on both the R and T wave peaks). With the offset of the complex designated as the beginning of the skip

region, however, a consistent skip region between complexes can be designated, thereby minimizing T wave picks.

The onset and offset search regions include the 150 msec preceding and following the PK-TOC, respectively. Assuming the PK-TOC to be the midpoint of the complex, the longest QRS duration of 200 msec (associated with a complete bundle branch block) would require twenty points to reach the onset and offset, respectively. The remaining ten points should then be sufficient to locate the offset (six consecutive first differences), as well as the onset (three consecutive first differences).

Searching for the onset or offset begins six points before or after the PK-TOC, respectively. Points in this region are assumed to be on the ascending or descending legs of the peak since the lower limit of the normal range of QRS duration is 30 msec. In addition, the skipped region prevents premature boundary location of complexes which have a low frequency, "plateaued" peak indicative of slowed or blocked conduction.

The number of consecutive differences less than the boundary tolerance to identify an onset or offset is determined by the duration of the preonset and postoffset (ST Segment) baseline, respectively. The preonset baseline duration (80 msec) is approximately two-thirds of the ST Segment duration (120 msec). Hence, a 20 msec interval (three qualifying consecutive differences) detects an onset while a 35 msec interval (six qualifying consecutive differences) detects an offset.

Since 16 percent MXDF represents the lowest frequency

ventricular depolarization, consecutive differences less than this tolerance would suggest that the points lie off the complex. There-fore, the first-pass onset, offset tolerance is set equal to 16 percent MXDF. The second-pass tolerance of 30 percent MXDF is used for bound-ary recognition when high frequency noise is superimposed on these areas. Of the total number of complexes, 109 percent were rejected because no onset was found while the offset location was estimated on .6 percent of the complexes.

## Skip Region

The purpose of a cardiac rate dependent skip region is to maximize a no-search region between complexes, thereby reducing the possibility of error and saving computing time. Four alternatives for skip region designation exist, depending on the heart rate.

The two critical heart rates for defining skip regions are 120 and 300 bpm, respectively. Special consideration for instantaneous heart rates greater than or equal to 300 was necessary to prevent nondetection of ventricular flutter and fibrillation waves. Using a 150 msec skip region from the PK-TOC caused the PK-REG (typically beginning at the skip index on the second complex search) to encom-pass the peaks of two complexes. However, with a 50 msec skip region from the PK-TOC, the PK-REG is confined to the following complex.

Complexes with an instantaneous rate exceeding 120 bpm (but less than 300 bpm) use a 150 msec skip region and rates less than or equal to 120 bpm use a 250 msec skip region. In theory, a forty point (200 msec) skip region from the PK-TOC for HR < 200, < 300, would be

sufficient to accommodate the minimum RR Interval (forty points) in
this rate category.  Complexes that are common to this rate category,
however, are typically lower frequency ventricular phenomena, i.e.,
qualifying difference < CTOLR60.  In practice, the qualifying differ-
ence is flagged in the second complex search on the prepeak leg of the
R (or S,T) wave peak, rather than on the peak itself.  A 150 msec skip
region from the PK-TOC, therefore, excludes the prepeak leg interval
for consecutive complexes with instantaneous RR Intervals equal to
or less than forty samples.

For RR Intervals between sixty and one hundred points, thirty
points is sufficiently small to accommodate the minimum RR Interval
in this rate category.  If the offset is detected at the upper limit
of the search region, approximately thirty points remain before the
next complex.  The decision to limit the skip region to fifty points
for rates < 120 per minute is necessary to prevent skipping over PVCs
which occur on the T wave (R on T phenomenon).  R on T PVCs can occur
any time after peak ventricular repolarization to the end of ventricu-
lar recovery.  The minimum RR Interval between a complex and a PVC
on its T wave in this data is forty-five points (225 msec), although
the normal interval from peak R wave to mid-T wave is 240 msec.
Therefore, fifty points is sufficiently small to prevent skipping an
R on T PVC in most cases.

<u>Justification of Noise Detection Criteria</u>

<u>Baseline Shift</u>

The ratio between the legs of a peak is a function of the

interval defining the legs. As discussed in the previous section, this interval should extend to the baseline to accurately represent the peak. Therefore, a minimum of ten points should be used, corresponding to a QRS duration of 100 msec.

The intent was to maximize the leg ratio while minimizing the number of rejections of valid complexes. To calculate this ratio, an analysis of the "worst case" peak is necessary, i.e., the R wave of a normal sinus beat with high ST Segment take-off. Leg ratios were calculated for 233 complexes having this morphology using a ten and twelve point interval, respectively. Figure 11 shows a histogram plotting the frequency of leg ratios as a function of the interval. Clearly, the maximum leg ratio with the minimum number of rejections occurs using a twelve point interval. A minimum leg ratio of .25 was chosen with an associated 4.3 percent FN rate.

## Maximum/Minimum Quantization

The maxima/minima noise algorithm is aimed at rejecting noise spikes that are not associated with a complex, or when associated, result in a small S/N ratio. On the other hand, multiple peak complexes should not be rejected as noise.

To empirically converge on the most robust set of values to satisfy these conditions, two types of complexes were examined. The right bundle branch block (RBBB) complex was chosen to represent the "worst case" multiple peak complex. Inherently, this complex can have up to five peaks representing the Q, R, S, R', and S' waves, respectively. In addition, this complex can be associated with a large,
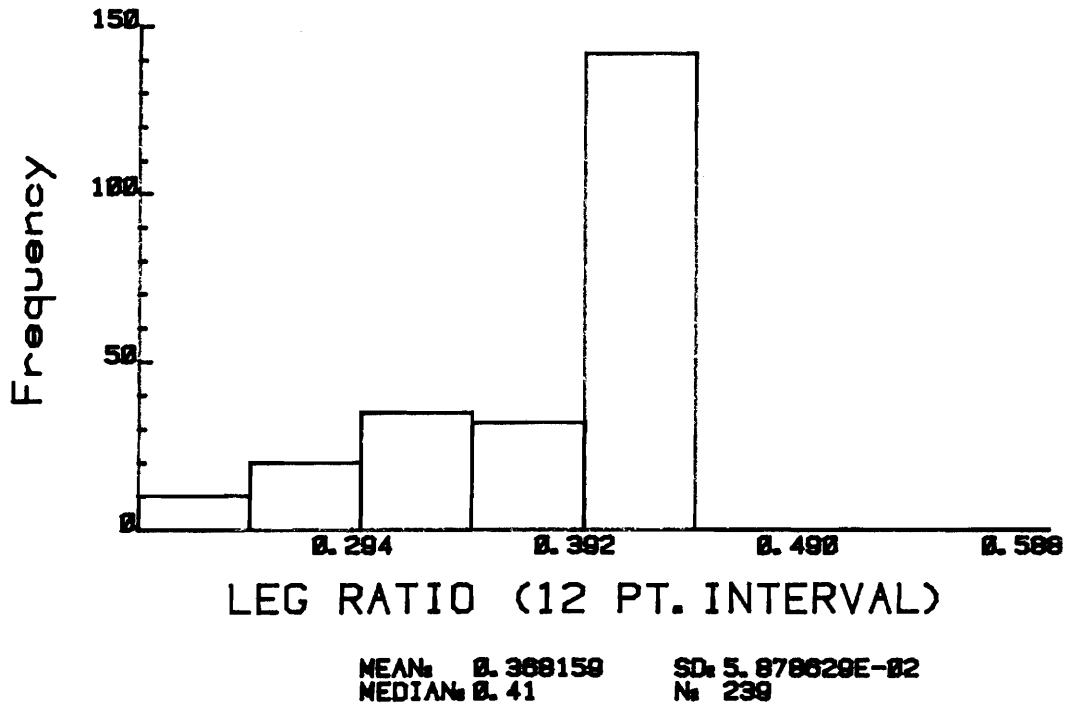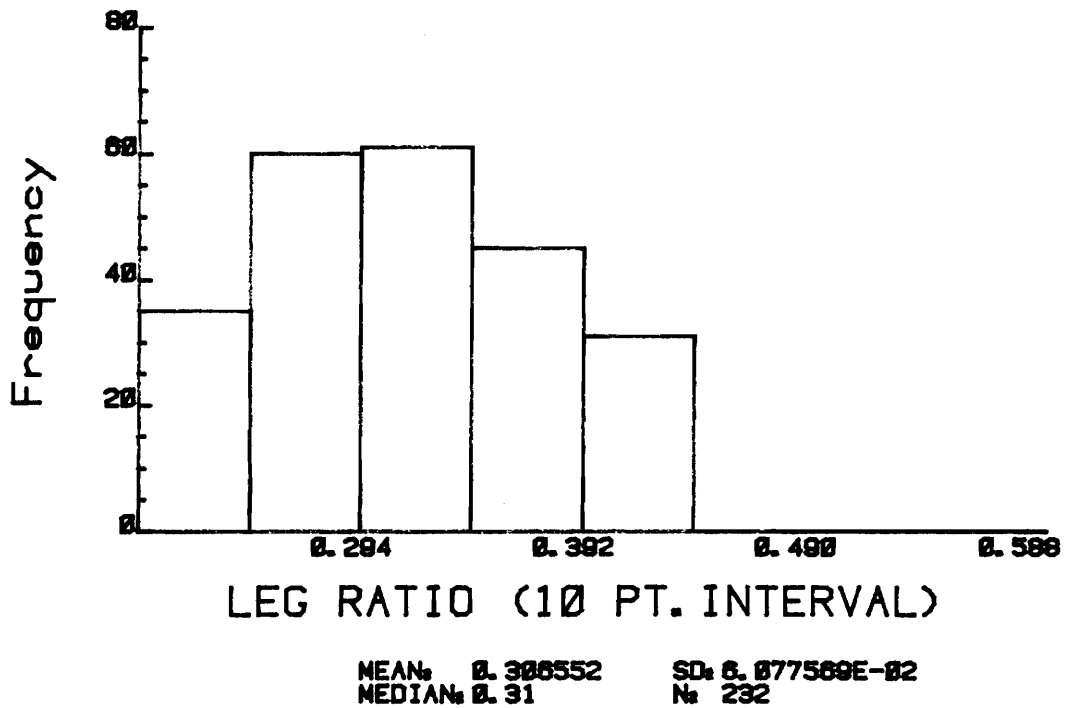
Fig. 11.  Frequency of prepeak, postpeak leg ratios using ten-
point and twelve-point intervals.

biphasic P wave bringing the possible number of peaks in the search region to seven. The other type of complex examined was the normal sinus complex contaminated with varying amplitudes of noise spikes. Of the 636 beats analyzed from four data files, 46 percent were RBBB complexes and 54 percent were contaminated normal sinus complexes.

Two trials were carried out with different values for the three criteria, i.e., percent S(i), maxima/minima search region, and the maxima/minima criteria were tallied for each set of values. The values chosen for each of the criteria are listed in Table 2 representing seventy-two different combinations. The weighted average error (AV(s)) was calculated for each combination of values:

TABLE 2

MAXIMUM/MINIMUM CRITERIA VALUES

| Percent S(i) | Maxima/Minima Search Region | Maxima/Minima Limit |
|---|---|---|
| Trial I | | |
| 8 | 20 | 6 |
| 10 | 30 | 7 |
| 15 | 40 | 8 |
| | | 10 |
| | | 12 |
| Trial II | | |
| 20 | 20 | 5 |
| 25 | 30 | 6 |
| 30 | 40 | 7 |

NOTE: S(i) = maximum absolute output to the peak detector.

$$AV(w) = \text{sum } (E(i) + IDX (i)) / IDX (total) \ i=1 \ to \ 4$$

where i represents the data files (A10150, B11580, C20440, E20310),
E the number of FNs, and IDX the number of indices. The four combina-
tions with the minimum error are presented in Table 3. Based on these
results, the optimal values for percent S(i), maxima/minima search
region, and the maxima/minima limit are 15, 150 msec, and 7,
respectively.

TABLE 3

MAXIMUM/MINIMUM WEIGHTED AVERAGE ERROR

| Percent (S(i) | Maxima/Minima Search Region | Maxima/Minima Limit | AV(w) |
|---|---|---|---|
| 15 | 30 | 7 | 1.1808 |
| 15 | 30 | 8 | 1.2013 |
| 15 | 40 | 8 | 1.1887 |
| 15 | 40 | 9 | 1.2013 |

NOTE: S(i) = maximum-absolute output to the peak-detection
detector; AV(w) = weighted average.

CHAPTER IV

RESULTS

This chapter is concerned with evaluating the performance of the QRS detection algorithm using a patient database collected in the LDS Hospital Coronary Care Unit. The algorithm, as described in Chapter II, was ultimately designed by successive identification and refinement of error sources. A final analysis was then performed using the criteria empirically determined to result in minimum QRS detection.

The evaluation of the test results can be divided into two phases:

1. Calculation of the error, sensitivity, and positive predictive accuracy of the algorithm

2. Examination of the causes of residual error.

Phase 1 is discussed in the next section followed by an analysis of the remaining error causes and their respective contribution to the total error.

## Calculation of Error, Sensitivity, and Positive Predictive Accuracy

The rate of beat misdiagnosis (false negative and false positive rates, respectively), correct beat diagnosis (sensitivity), and positive predictive accuracy were calculated, given the respective

frequencies of true positives (TPs), false negatives (FNs), and false positives (FPs) (see Table 4). All visually verified peak time of occurrences in the patient data files, without regard to wave configuration, represent the total number of actual QRS complexes in the data. The number of true complexes detected by the algorithm represent the true positives, complexes not labeled as such represent the false negatives, and noncomplexes detected as complexes represent the false positives. One of two verdicts was possible for each complex in the data, i.e., positive or negative. A positive test result indicated a valid beat affirmation by the algorithm, while a negative test result indicated an invalidation of the beat candidate.

By comparing the true diagnosis to the results of the test, the rate of TPs (TPR, or sensitivity), FNs (FNR), and FPs (FPR) were calculated. The rate of correctly (TPR) and incorrectly (FNR and FPR) diagnosed complexes are listed in Table 4. Of a total of 7,205 QRS complexes in the database, the rate of FN and FP error is .0359 and .0071, respectively, the sensitivity .9641, and the positive predictive accuracy .9573 (see Table 4 for calculations).

## Causes of Error

An investigation of the causes of the error is important since the statistical results are dependent upon the type of rhythm disturbances and the amount of noise superimposition in the data.

The principal cause of false negative and false positive error is noise spike contamination, due to the superimposition of muscle artifact on the waveform. Excessive noise spike superimposition accounts for 84.17 and 92.16 percent of the FN and FP outcomes,

TABLE 4

TEST RESULTS

| Number | Test | | Total |
|---|---|---|---|
| | + | - | |
| TP | 6,946 | 259 | 7,205 |
| TN | 51 | | |
| Total | 6,997 | | |

NOTE:   FNR = FN/TP + FN = 259/7,205 = .0359; FPR = FP/TP + FN = .0071; TPR = TP/TP + FN = 6,946/7,205 = .9641; Positive Predictive Accuracy = TP/TP + FP + FN = 6,946/6,997 + 259 = .9573.

respectively.  FNs induced by noise (FN(ns)) are those beats rejected because of excessive muscle artifact superimposed on the complex. Even to the trained cardiologist, the task of identifying ventricular activity in such waveforms is difficult and uncertain, rendering the signal "unprocessable."  FPs attributed to such noise (FP(ns)) are typically caused by isolated noise spikes or a larger amplitude noise spike relative to adjacent smaller amplitude noise spikes.

The remaining error is caused by variant QRS morphologies which qualify the candidate as noise.  These invalid candidate rejections are caused by QRS waveforms qualifying as a shift in baseline, sudden cardiac rate changes which can cause a complex search region or skip region malfunction, limitation of the polarity comparison algorithm in ventricular flutter-fibrillation, or insufficient gain which results in a low S/N ratio.

Table 5 justifies the occurrence of all false negative and

TABLE 5

CAUSES OF ERROR

| Causes | Number of Candidates | Percent of Error |
|---|---|---|
| False Negative Error | FN (259) | FN (Total) |
| Excessive Noise Spike Superimposition (FN(ns)) | 218 | 84.17 |
| Baseline Shift (FN(bs)) | 25 | 9.65 |
| Complex Search Region (FN(cr)) | 6 | 2.32 |
| Skip Region (FN(sr)) | 4 | 1.54 |
| Polarity Comparison (FN(pc)) | 3 | 1.16 |
| Low Gain (FN(lg)) | 3 | 1.16 |
| False Positive Error | FP (51) | FP (Total) |
| Excessive Noise Spike Superimposition (FP(ns)) | 47 | 92.16 |
| FN-Induced FP (FP(fn)) | 4 | 7.84 |

false positive error, respectively, and tabulates the percent of total

error each cause represents. An analysis of the critical noise voltage

level for the acceptance/rejection of a candidate contaminated by

noise spike superimposition is examined initially, followed by an

in-depth investigation of the remaining causes of false negative and

false positive error, respectively.

Critical Voltage for Noise
Spike Rejection

The level of muscle artifact interference can be measured in

terms of root mean square (RMS). Beats rejected because of excessive

noise spike contamination (FN(ns)) were examined to assess the critical

RMS voltage above which the candidate is rejected as being too noisy.

The RMS value represents the average voltage defined over one period, and is calculated from the formula:

$$RMS(i) = (sum ((X(i) - X(m)))^2 / n / k )^{\frac{1}{2}} \quad i=1 \text{ to } n$$

where n is the number of samples in one period, X(m) the mean of the samples X(1), X(2), ...X(n), and k the number of periods.

Twenty-seven false negatives chosen from the set of FN(ns)s that were rejected because of violation of the maximum/minimum criteria (i.e., summation of extrema > 7) were viewed on the Tektronix graphics terminal to identify period(s) of extrema. A period is defined as a sequence of maximum-minimum-maximum or minimum-maximum-minimum, and must satisfy the following criteria:

1. The period must not include the QRS complex.

2. The period must occur within the maxima/minima search region.

Knowing the instantaneous values of valid periodic extrema, an RMS voltage (RMS(i)) was calculated and the maximum absolute output to the peak detector (S(i)) recorded.

Since the RMS(i) values are a function of the S(i), a linear regression was done. The regression equation was computed using the following formula:

$$Y(i) = b_0 X(i) - b_1$$

where $b_0$ and b equal:

$$b_0 = sum \ (X(i) - X(m)) \ (Y(i) - Y(m)) \ / \ sum \ (X(i) - X(m))^2$$

$$b = Y(m) - b_0 X(m)$$

with X representing the S(i) values, Y the RMS(i) values, X(m) the mean of samples X(1), X(2) ... X(27), and Y(m) the mean of samples Y(1), Y(2) ... Y(27).

The calculated regression equation is:

$$RMS(i) = .095 \ S(i) - .049 \ .$$

A plot of the regression line and the RMS(i) and S(i) values are shown in Figure 12.

The sample correlation coefficient (r) was calculated using the equation:

$$r = sum \ (X(i) - X(m)) \ (Y(i) - Y(m))/$$

$$(sum \ (X(i) - X(m))^2 * sum \ (Y(i) - Y(m))^2)^{\frac{1}{2}} \ .$$

The calculated value of r is .844.

To test whether r is statistically significant, a test of the null hypothesis, r = 0, was done. Using Table 5A in Statistical Methods in Medical Research (Armitage, 1977) and n-2 degrees of

$$Y = 0.096*X - 0.053 \quad R^2 = 0.84$$
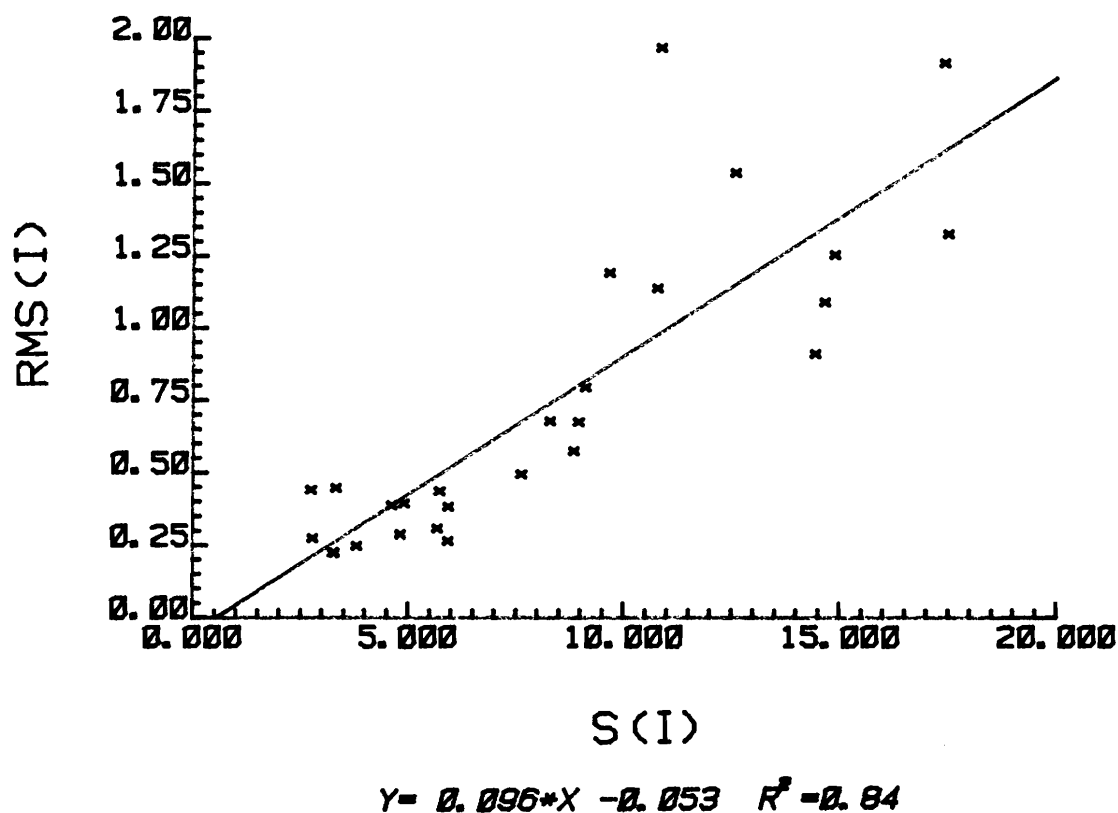
Fig. 12. Linear regression plot of noise vs. peak detector output in mv.

freedom, the null hypothesis can be rejected at a significant level of 0.001 for r values > .597. Hence, there is predictive value in using this regression equation for determining the critical RMS values for acceptance/rejection of beats contaminated with noise spikes.

## False Negative Error

Baseline shift rejection. Baseline shift rejection accounts for 9.65 percent of the total FN error. In theory, candidates with a minimum leg amplitude less than 25 percent of the maximum leg amplitude are considered to be a shift in baseline due to patient movement

rather than a complex. However, three types of complexes can have (max S(i)) peak configurations with leg ratios less than .25. These complexes include:

1. Ventricular flutter waves

2. R waves with elevated ST Segment

3. RBBB complexes.

Typically, these rejections are wide peaks, i.e., prolonged wave duration which manifest from slowed or blocked conduction in localized regions of the ventricles. The sinusoidal configuration inherent to the R and T wave of a ventricular flutter wave is the result of slowed impulse conduction through the ventricular myocardium rather than the specialized Purkinje network. The R wave morphology (associated with ST Segment elevation) and the configuration of the R' or S' wave of an RBBB complex are the result of blocked conduction imposed by an infarcted region in the left ventricle and the right bundle branch of the right ventricle, respectively.

Ventricular flutter waves (6.15 percent, total) were rejected as baseline shift because the leg ratio of the peak R or T wave was less than .25. Ventricular flutter is produced by a ventricular ectopic focus discharging at a rate of 200-300 impulses per minute. The ventricular "contractions" elicited at rates exceeding 250 bpm, however, are the most vulnerable to baseline shift rejection. As the rate of discharge increases, the ability of the partially depolarized ventricular cells to initiate an Na-dependent action potential becomes progressively more inhibited. The result is a reduction in peak to peak amplitude (i.e., R to T) and a widening of peak morphology due to

the impaired, slow-rising action potential. This wide peak configuration can qualify the candidate as a shift in baseline.

An acute or recent myocardial infarction can cause the ST Segment to rise above the baseline resulting in a premature leveling (beginning at the j point) of the descending leg of the R wave peak. Hence, the amplitude of the descending leg decreases as the slope of the ST Segment (included in the leg interval) decreases. FN(bs)s caused by R waves with high ST Segment take-off account for 60.00 percent of the FN(bs) total; however, only 4.30 percent of the total number of candidates exhibiting this phenomenon were rejected by the baseline shift criteria. Remember that this FN rate was chosen as a trade-off between maximizing the leg ratio and minimizing the number of FNs.

Baseline shift rejection of RBBB complexes is an infrequent phenomenon occurring in only 1.06 percent of all RBBB complexes. Infarcted regions of the right bundle branch, however, can cause widening of the R' or S' wave (depending on the location of the infarct). Those waves which encompass the infarct on one of two legs, but not both, can be rejected if the infarcted leg amplitude is sufficiently reduced from the other (maximum) leg amplitude.

Complex search region and skip region rejection. A reduction in the RR Interval from the average RR Interval can cause the complex search region (CPLX-REG) to include more than one complex or the skip region (SKP-REG) to include a TP. Skip region omissions (FN(sr)) are caused by large changes in consecutive RR Intervals; however, the majority of FNs caused by cardiac rate changes are due to the failure of the CPLX-REG to include only one TP in the designated region when

an increase in heart rate occurs. These search and skip region mal-
functions account for 3.86 percent of the FN(nn) and are examined
individually.

Complex search region rejection. Remember that the CPLX-REG is
designated as two-thirds of twice the average RR Interval calculated
over the initial ten complexes. If a 50 percent or more increase in
the average RR Interval occurs, then the CPLX-REG can encompass more
than one TP. The problem arises when the complexes included in the
CPLX-REG present at different frequencies, i.e., at least one complex
has a qualifying difference greater than CTOLR60 (a first search
phenomenon) with at least one complex less than CTOLR60 (a second
search phenomenon). When a second search phenomenon precedes a first
search phenomenon in the same CPLX-REG, the former is not detected.

Episodes of consecutive complexes which tend to represent
second to first-search transitions include sinus capture of second
search phenomena (generally ventricular tachycardia, flutter, or
fibrillation), consecutive ventricular flutter waves, deterioration
of ventricular flutter into ventricular fibrillation, and consecutive
multifocal PVCs. Ectopic ventricular depolarizations can be first or
second-search phenomena, although they are typically the latter since
the route of depolarization is via the slower-conducting ventricular
myocardium.

Skip region rejection. Skip region omissions are caused by
changes in consecutive RR Intervals from one rate category to the next.
Fifty percent of the FN(sr) are attributable to the inclusion of an R
on T PVC in the skip region when a rate change from less than 120 bpm

(normal sinus complex) to 199-299 bpm (PVC) occurs. Since an ectopic focus discharging during ventricular repolarization can occur at any heart rate, the 120 bpm or less rate category is the most vulnerable to omission of an R on T PVC. The designated skip region for this rate category (250 msec), however, was chosen as a compromise between maximizing the skip region and minimizing skip region omissions. An FN error (total) of less than 1 percent (.77 percent) was the result of skip region omission of R on T PVCs.

Consecutive ventricular flutter waves are particularly vulnerable to skip region omission since instantaneous heart rates in a flutter sequence alternate between the 199-299 and greater than 299 bpm rate categories. A decrease in consecutive RR Intervals from forty to sixty to less than forty points can cause the nondetection of the "early" complex if the prepeak interval amplitude containing a qualifying first difference is included in the 150 msec skip region.

The final source of FN(cr) is the lack of a positive test (i.e., TP and FP) in a previous CPLX-REG. If the complexes preceding and following the FN are detected (TP1 and TP2, respectively), TP2 is subject to an offset search since its "RR Interval" is greater than sixty, i.e., actually encompasses two heart cycles. This search, in turn, can cause omission by skip region inclusion of the complex following TP2.

Figure 13 shows a sequence of four complexes whereby the first and third complexes are detected and the second complex is an FN. Assuming the RR Interval to be the same for TP1-FN (RR1), FN-TP2 (RR2), and TP2-TP3 (RR3), a minimum "heart rate" of 400 bpm (RR = 30)
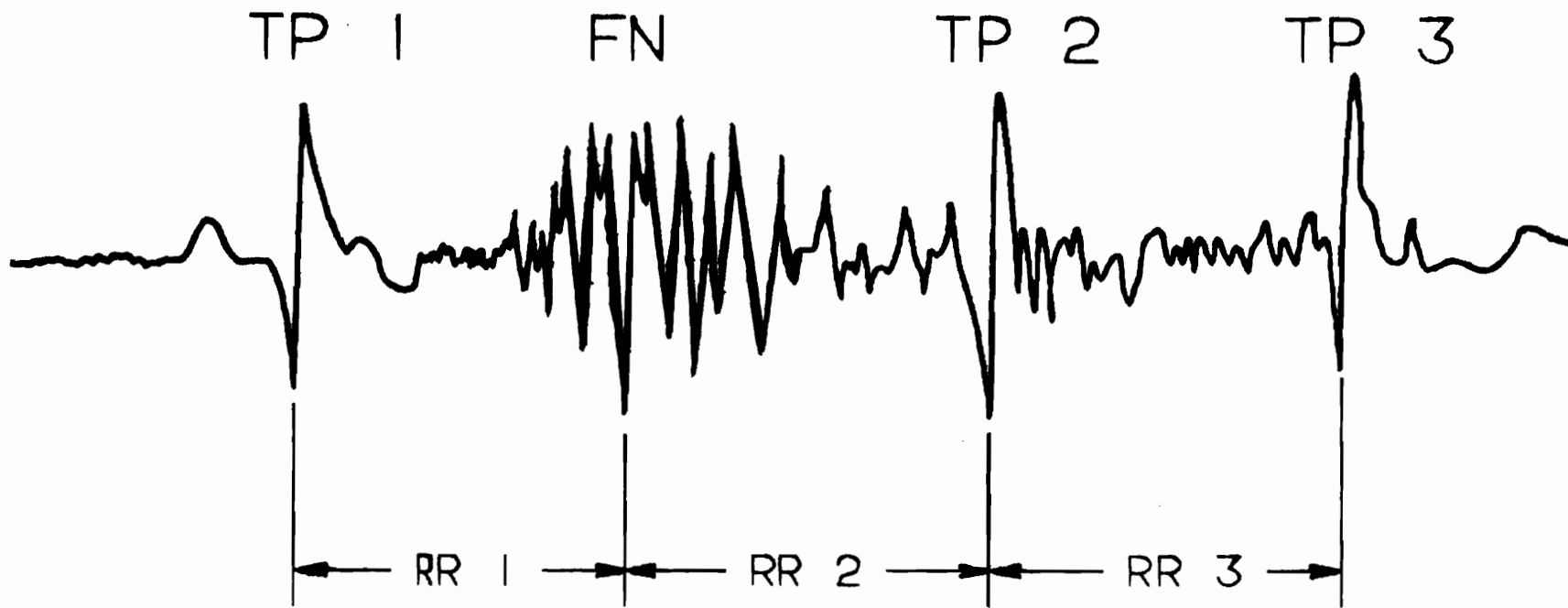
Fig. 13. False negative caused by skip region omission.

would be necessary to exempt TP2 from an offset search. Therefore, assuming that the RR Intervals are equal (RR1 = RR2 = RR3) and that the end of TP2 was located at the upper--"worst case" limit--i.e., twenty four points from the PK-TOC, all FNs with RR Intervals between thirty and seventy-five (corresponding to a rate of 160-400 per minute) would qualify an offset search for TP2 and subsequent rejection of the next complex (TP3). Twenty-five percent of the FN(sr)s are caused by the nonvalidation of a candidate in a CPLX-REG, i.e., FN-induced.

Polarity comparison rejection. As mentioned previously, with rapid ventricular rates (250-300 per minute), it is difficult to consistently detect either the R or T wave; however, the nondetection of a beat by T wave recognition can occur. If the peak detection in a flutter sequence begins with the R wave and the following T wave represents a maximum $S(i)$ peak, then the T wave will be rejected by polarity and the complex will not be detected. Seven and one-third (7.33) percent of the FN(nn) are caused by polarity rejection of the T wave in a ventricular flutter sequence.

Low gain rejection. A low gain signal makes it particularly difficult to discriminate noise from actual ventricular activity. For instance, 15 percent of the peak detector output used for maxima/minima quantization can approach such a small magnitude that rejection of valid complexes can occur. In addition, it is highly probable that low amplitude ectopic beats will not be flagged due to the small deflection from baseline. Rejection caused by a low gain signal in this analysis accounts for 1.16 percent of FN(nn).

False Positive Error

   False negative-induced false positive.  The FP error attributable
to the occurrence of a previous FN (FP(fn)) is caused by the rejection
of a first-pass true positive candidate whose morphology represents
a P-QRS sequence.  On the second-pass search, the P wave can be
detected, constituting an FN-induced FP.  Typically, lower frequency
ventricular contractions are not preceded by a P wave since the
depolarizing wave is initiated and propogated in the ventricular
myocardium and not the specialized conduction system.  Therefore,
second-pass P wave detection is seen only in complexes which are
initiated from an atrial focus.

DISCUSSION AND CONCLUSION

This research project was proposed to design a QRS detection algorithm which could accurately detect ventricular activity in contaminated single lead electrocardiographic data. The algorithm did not include classifying the beat as normal or abnormal. The reason for undertaking such a research endeavor is because most automated rhythm monitoring systems, including the system currently in use at the LDS Hospital CCU, report unacceptably high error rates. The majority of error has been reported to be the result of misclassification of signal artifact as ventricular activity or failure to identify the beat because of rejection of noisy segments of data. The goal of this research was to minimize this error due to noise misclassification in an attempt to provide a more clinically useful automated arrhythmia monitoring system.

To insure that the algorithms could function accurately and reliably in noise contaminated data, over 90 percent of the developmental data base was contaminated with noise. In addition, a wide array of rhythm disorders were included, particularly those labeled as potentially dangerous to the patient. The initial phase involved identifying a reference point on each complex in the data by visual inspection. An attempt was then made to converge on a set of criteria which generated minimum QRS detection error over all the data complexes

files. The error was reported in terms of the FPR (.0071) and FNR (.0359); the ability of the algorithm to detect ventricular activity was expressed in terms of sensitivity (.9641) and positive predictive accuracy (.9573), respectively.

Because the algorithm development was performed off-line on a selective data base gathered in the CCU at the LDS Hospital, it is difficult to assess how well the criteria would function in a real-time monitoring environment. Furthermore, a comparison of the reported error in the system currently in use in the LDS Hospital CCU and the results of this criteria is difficult since the former error was reported in terms of false alarms. The major cause of error reported in the LDS CCU system evaluation was attributed to signal artifact. It was the consensus that the error was incurred in the QRS detection phase rather than the classification phase of analysis. Since a low FPR was reported in this analysis using a heavily noise contaminated data base, it can be concluded that this QRS detection/delineation algorithm shows a substantial improvement over the current system.

The key to designing accurate beat recognition criteria was in realizing that the most significant problem confronting automated rhythm analysis is signal artifact and that liberal rejection of noisy segments of data and toleration of high FPRs to minimize the risk of FNs is not a good solution to the noise problem in the clinical monitoring environment. Most systems identify the QRS complex by some variation of the derivative technique and assume that this is sufficient to validate the presence of ventricular activity. The first

automated rhythm monitoring programs used a high threshold to minimize the incidence of FPs while subsequent programs have used low thresholds to minimize the number of FNs. However, this approach is invariably at the expense of increasing the incidence of the other. Other systems use limited noise detection criteria to identify the presence of muscle artifact and then suspect analysis upon detection. The majority of rhythm analysis systems, however, neglect to include noise detection criteria in the QRS recognition phase.

The approach taken in this project is a unique one in that a candidate must satisfy numerous noise detection criteria before validation. An inclusive derivative search (i.e., a dual scan) was used to initially detect all possible candidates. The beat candidates were then subject to passage of noise detection algorithms for validation as a QRS complex. The noise criteria have shown to be effective in minimizing the incidence of FPs in the candidate set without a substantial increase in FNs. The high FN rate relative to the FP rate can be attributed to excessive muscle artifacts superimposed on over 90 percent of the data, rendering it unprocessable even to the trained cardiologist. Furthermore, a false negative error rate of 3.59 percent (percent total beats) reported in this analysis is small in comparison to results published in evaluations of rhythm monitor's performance in the literature (see Chapter I).

The algorithm used to quantitate the maxima and minima to determine the level of noise spike superimposition is used in a few detection schemes, of which ARGUS is one. An S/N approach to counting extrema for defining acceptable/unacceptable noise levels was first

proposed by Pryor (1972) in his dissertation titled "Automated Computer Analysis of the Electrocardiogram." This approach is more effective than simply quantitating extrema without taking into consideration the amplitude of the noise spikes in relation to the dominant peak in the complex. Simple extrema counts ultimately result in high data losses as reported in evaluations of automated rhythm monitoring systems using this technique. This approach has improved the S/N technique for maxima/minima quantitation described by Pryor. First of all, a lower S/N ratio is tolerated, i.e., S/N ratio < 6.67 as compared to an S/N ratio < 10 proposed by Pryor. Second, the signal is defined as the output to a weighted convolution equation rather than the change in amplitude between the maximum and minimum QRS value. Also, a symmetrical search region for maxima/minima quantization was used since the one-sided search used by Pryor (i.e., 250 msec backwards) can overlap into the previous QRS complex region in high heart rates.

Two original algorithms designed to identify manifestations of noise were put forth in this project. Both capitalize on inherent morphologic discrepancies between artifact and QRS complex morphology.

The initial algorithm was designed to detect shifts in baseline. Baseline shifts are a frequent occurrence in monitored electrocardiographic data, and in the author's opinion constitute an underestimated source of FP error in automated rhythm analysis systems. In evaluations of other systems there is no reported attempt to identify shifts in baseline per se, although there are limited filtering techniques designed to reduce their impact. Despite the lack of hard

data to assess the frequency of candidates rejected as baseline shifts in this research, the number of maxima/minima rejections were superceded by baseline shift rejections. This is not surprising in light of the excessively noisy data base used in the analysis and the attempt to minimize the data loss due to noise spike contamination, but it does imply that a high percentage of FPs in the initial candidate set were shifts in baseline. In retrospect this algorithm has improved the sensitivity at the expense of a small number of FNs.

A second algorithm restricts the interval of samples correlating most highly to a peak configuration. If a nonpeak is identified, then the candidate is rejected as nonventricular activity. This approach was effective in rejecting large intervals of high frequency (ascending or descending) shifts in baseline, even though these shifts did not occur as frequently as smaller amplitude shifts in baseline. FNs rejected as nonpeaks occurred only when there was insufficient gain or the signal was part of a cascading or ascending shift in baseline.

Areas of vulnerability in this QRS detection/delineation algorithm can be strengthened by improving existing algorithms and developing new discriminative criteria. Improvement of existing algorithms could result in a reduction of false positive error, although the overriding consideration is to reduce the incidence of false negatives. A possible reduction in the allowable S/N ratio to further minimize the data loss is possible, although it is probable that it would result in an increase in classification error. The philosophy of flexible skip regions based on the heart rate could be

search region designation. The small incidence of error due to the inclusion of more than one complex in the complex search region can be prevented by designating its range based on the instantaneous RR Interval or a "selective" averaged RR Interval. In addition, passage of other criteria could be required before a baseline shift rejection is definitive. For example, if the candidate identified as a shift in baseline was part of a fast ventricular sequence, then the allowable leg ratio could be reduced, thereby preventing the rejection of some ventricular tachycardiac, flutter, and fibrillation beats.

The problem of isolated noise spike detection remains to be the most significant source of FP error in this project. New algorithms need to be developed to identify the presence of noise not associated with a beat, although this is difficult in rhythm monitoring analysis since consecutive RR Intervals can be markedly irregular and noise spikes often have the same configuration as a QRS complex. This source of FP error could possibly be reduced in the classification phase of the analysis.

As a proposal of continuation, the next phase in this research project would be to add a classification scheme so that cardiac rhythm could be diagnosed. This would require development of diagnostic logic for single and multibeat pattern recognition.

Ultimately the real value of this research project will depend on how well the QRS detection/delineation algorithm functions in a clinical monitoring environment. Hence, this project represents only the first step in the analysis of cardiac rhythm and has shown that

ventricular activity, even in the presence of noise, can be detected

by a computer with minimal error.

SELECTED BIBLIOGRAPHY


Amazeen, P. G.; Moruzzi, R. L.; and Feldman, C. L. "Phase Detection
    of R Waves in Noisy Electrocardiograms." IEEE Transactions on
    Bio-Medical Engineering BME 19 (January 1972):63-66.

Armitage, P. Statistical Methods in Medical Research. Oxford:
    Blackwell Scientific Publications, 1977.

Arnold, J. M.; Shah, P. M.; and Clarke, W. B. "Artifact Rejection in
    a Computer System for the Monitoring of Arrhythmias." Computers
    in Cardiology Conference (1975):163-167.

Balda, R. A.; Diller, G.; Deardorff, E.; Dove, J.; and Hsieh, P.
    "The HP ECG Analysis Program." Edited by J. H. van Bemmel,
    and J. L. Willems, Trends in Computer-Processed Electrocardio-
    grams. New York: Elsevier North-Holland Biomedical Press,
    1977.

Berson, A. S.; Ferguson, T. A.; Batchlor, C. D.; Dunn, R. A.; and
    Pipberger, H. V. "Filtering and Sampling for Electrocardio-
    graphic Data Processing." Computers and Biomedical Research
    10 (1977):605-616.

Birman, K. P. "Rule-Based Learning for More Accurate ECG Analysis."
    IEEE Transactions on Pattern Analysis and Machine Intelligence
    PAMI-4 (July 1982):369-380.

Cox, J. R.; Nolle, F. M.; and Arthur, R. M. "Digital Analysis of the
    Electrencephalogram, the Blood Pressure Wave, and the Electro-
    cardiogram." Proceedings of the IEEE 60 (October 1972):1137-
    1164.

Day, H. W., and Averill, K. "Recorded Arrhythmias in an Acute
    Coronary Care Area." Diseases of the Chest 49 (February 1966):
    113-118.

Engelse, W. A. H., and Zeelenberg, C. "A Single Scan Algorithm for
    QRS Detection and Feature Extraction." Computers in Cardio-
    logy Conference (1979):37-42.

Feldman, C. L.; Amazeen, P. G.; Klein, M. D.; and Lown, B. "Computer
    Detection of Ventricular Ectopic Beats." Computers and Bio-
    medical Research 3 (1971):666-674.

Feldman, C. L. "Trends in Computer ECG Monitoring." Edited by J. H. van Bemmel, and J. L. Willems, Trends in Computer-Processed Electrocardiograms. New York: Elsevier North-Holland Biomedical Press, 1977.

Flynn, R. L., and Fox, S. M. "A Coronary Care Concept." Proceedings of the New England Cardiovascular Society 24 (1965-66):24-26.

Fozzard, H., and Kinias, P. "Computers for Recognition and Management of Arrhythmias." Medical Clinics of North America 60 (March 1976):291-298.

Frankel, P.; Rothmeier, J.; James, D.; and Quaynor, N. "A Computerized System for ECG Monitoring." Computers and Biomedical Research 8 (1975):560-567.

Frost, D. A.; Yanowitz, F. G.; and Pryor, T. A. "Evaluation of a Computerized Arrhythmia Alarm System." The American Journal of Cardiology 39 (April 1977):583-587.

Geddes, J. S., and Warner, H. R. "A PVC Detection Program." Computers and Biomedical Research 4 (1971):493-508.

Geltman, E. M.; Ehsani, A. A.; Campbell, M. K.; Schechtman, K.; Roberts, R.; and Sobel, B. E. "The Influence of Location and Extent of Myocardial Infarction on Long-Term Ventricular Dysrhythmia and Mortality." Circulation 60 (October 1979): 805-814.

Golden, D. P.; Wolthuis, R. A.; and Hoffler, G. W. "A Spectral Analysis of the Normal Resting Electrocardiogram." IEEE Transactions on Biomedical Engineering BME-20 (September 1973):366-372.

Haywood, L. J.; Harvey, G. A.; and Kirk, W. L. "On-line Digital Computer for Electrocardiogram Monitoring in a Coronary Care Unit." Journal of the Association for the Advancement of Medical Instrumentation 3 (September 1969):165-169.

Haywood, L. J.; Murphy, V. K.; Harvey, G. A.; and Saltzberg, S. "On-Line Real Time Computer Algorithm for Monitoring the ECG Waveform." Computers and Biomedical Research 3 (1970):15-25.

Himmelhoch, S. R.; Dekker, A.; Gazzaniga, A. B.; and Like, A. A. "Closed-Chest Cardiac Resuscitation: A Prospective Clinical and Pathological Study." New England Journal of Medicine 270 (January 1964):118-122.

Hochberg, H. M.; Weihrer, A. L.; McAllister, J. W.; Calatayud, J. B.; Zimmerman, A. K.; and Caceres, C. A. "Monitoring of Electrocardiograms in a Cornary Care Unit by Digital Computer." The Journal of the American Medical Association 207 (March 1969): 2421-2424.

Holsinger, W. P.; Kempner, K. M.; and Miller, M. H. "A QRS Preprocessor Based on Digital Differentiation." IEEE Transactions on Bio-Medical Engineering BME-18 (May 1971):212-217.

Jenkins, J. M. "Automated Electrocardiography and Arrhythmia Monitoring." Progress in Cardiovascular Disease 25 (March/April 1983):367-408.

Julian, D. G.; Valentine, P. A.; and Miller, G. G. "Disturbances of Rate, Rhythm, and Conduction in Acute Myocardial Infarction. A Prospective Study of 100 Consecutive Unselected Patients with the Aid of Electrocardiographic Monitoring." The American Journal of Medicine 37 (December 1964):915-927.

Katz, A. M. Physiology of the Heart. New York: Raven Press, 1980.

Killip, T. "Impact of Coronary Care on Mortality from Ischemic Heart Disease." Proceedings of the Conference on the Decline in Coronary Heart Disease Mortality, Bethesda, October 1978.

Killip, T., and Kimball, J. T. "Experiences with Monitoring Myocardial Infarction at the New York Hospital-Cornell Medical Center: Comparison of Regular Hospital Care and Coronary Unit Care." Proceedings of the New England Cardiovascular Society 24 (1965-66):27-29.

Knoebel, S. B.; Rasmussen, S.; Lovelace, D. E.; and Anderson, G. J. "Nonparoxysmal Junctional Tachycardia in Acute Myocardial Infarction: Computer-Assisted Detection." The American Journal of Cardiology 35 (June 1975):824-830.

Lown, B.; Fakhro, A. M.; Hood, W. B.; and Thorn, G. W. "The Coronary Care Unit: New Perspectives and Directions." The Journal of the American Medical Association 199 (January 1967):156-166.

Lown, B.; Vassaux, C.; Hood, W. B.; Fakhro, A. M.; Kaplinsky, E.; and Roberge, G. "Unresolved Problems in Coronary Care." The American Journal of Cardiology 20 (October 1967):494-508.

Macy, J., and James, T. N. "The Value and Limitations of Computer Monitoring in Myocardial Infarction." Progress in Cardiovascular Diseases 13 (March 1971):495-505.

Margolis, J. R., and Wagner, G. S. Coronary Care: Arrhythmias in Acute Myocardial Infarction. Dallas: American Heart Association, Inc., 1976.

Mead, C. N.; Clark, K. W.; Potter, S. J.; Moore, S. M.; and Thomas,
L. J. "Development and Evaluation of a New QRS Detector/
Delineator." Computers in Cardiology Conference (1979):251-
254.

Nolle, F. M. "ARGUS, A Clinical System for Monitoring Electrocar-
diographic Rhythms." Ds.C. Dissertation, Washington University,
1972.

Nolle, F. M. "The ARGUS Monitoring System: A Reappraisal." Edited
by J. H. van Bemmel, and J. L. Willems, Trends in Computer-
Processed Electrocardiograms. New York: Elsevier North-
Holland Biomedical Press, 1977.

Oliver, G. C.; Nolle, F. M.; Wolff, G. A.; Cox, J. R.; and Ambos, H.
D. "Detection of Premature Ventricular Contractions with a
Clinical System for Monitoring Electrocardiographic Rhythms."
Computers and Biomedical Research 4 (1971):523-541.

Pipberger, H. V.; Dunn, R. A.; and Berson, A. S. "Computer Methods
in Electrocardiography." Annual Review of Biophysics and
Bioengineering 4 (1975):15-42.

Pipberger, H. V.; McCaughan, D.; Littmann, D.; Pipberger, H. A.;
Cornfield, J.; Dunn, R. A.; Batchlor, C. D.; and Berson, A. S.
"Clinical Application of a Second Generation Electrocardio-
graphic Program." The American Journal of Cardiology 35 (May
1975):597-608.

Pryor, T. A. "A Note on Filtering Electrocardiograms." Computers
and Biomedical Research 4 (1971):542-547.

_____. "Computerized Analysis of the ECG." Ph.D. dissertation,
The University of Utah, 1972.

Romhilt, D. W.; Bloomfield, S. S.; Chou, T.; and Fowler, N. O.
"Unreliability of Conventional Electrocardiographic Monitoring
for Arrhythmia Detection in Coronary Care Units." The American
Journal of Cardiology 31 (April 1973):457-461).

Rosenberg, H. M., and Klebba, A. J. "Trends in Cardiovascular Mor-
tality with a Focus on Ischemic Heart Disease: United States,
1950-1976." Proceedings of the Conference on the Decline in
Coronary Heart Disease Mortality, Bethesda, October 1978.

Sanders, W. J.; Alderman, E. L.; and Harrison, D. C. "The Development
of a 'second generation' ECG Monitoring System." Edited by
J. H. van Bemmel, and J. L. Willems, Trends in Computer-
Processed Electrocardiograms. New York: Elsevier North-Holland
Biomedical Press, 1977.

Shah, P. M.; Arnold, J. M.; Haberern, N. A.; Bliss, D. T.; McClelland, K. M.; and Clarke, W. B. "Automatic Real-Time Arrhythmia Monitoring in the Intensive Coronary Care Unit." The American Journal of Cardiology, 39 (May 1977):701-708.

Spann, J. F.; Moellering, R. C.; Haber, E.; and Wheeler, E. O. "Arrhythmias in Acute Myocardial Infarction. A Study Utilizing an Electrocardiographic Monitor for Automatic Detection and Recording of Arrhythmias." New England Journal of Medicine 271 (August 1964):427-431.

Stallman, F. W., and Pipberger, H. V. "Automatic Recognition of Electrocardiographic Waves by Digital Computer." Circulation Research 9 (November 1961):1138-1143.

Steinberg, C. A.; Abraham, S.; and Caceres, C. A. "Pattern Recognition in the Clinical Electrocardiogram." IRE Transactions on Bio-Medical Electronics BME-9 (1962):23-30.

Swenne, C. A.; Duisterhout, J. S.; and van Hemel, N. M. "Interactive Computerized CCU-Monitoring." Edited by J. H. van Bemmel, and J. L. Willems, Trends in Computer-Processed Electrocardiograms. New York: Elsevier North-Holland Biomedical Press, 1977.

Vetter, N. J., and Julian, D. G. "Comparison of Arrhythmia Computer and Conventional Monitoring on Coronary-Care Unit." The Lancet 9/24 (May 1975):1151-1161.

Wartak, J.; Milliken, J. A.; and Karchmar, J. "Computer Program for Pattern Recognition of Electrocardiograms." Computers and Biomedical Research 4 (1970):344-374.

Whalen, R. E.; Ramo, B. W.; and Wallace, A. G. "The Value and Limitation of Coronary Care Monitoring." Progress in Cardiovascular Diseases 13 (March 1971):422-436.

Wolthuis, R. A.; Froelicher, V. F.; Hopkirk, A.; Fischer, J. R.; and Keiser, N. "Normal Electrocardiographic Waveform Characteristics During Treadmill Exercise Testing." Circulation 60 (November 1979):1028-1035.

Yanowitz, F.; Kinias, P.; Rawlings, D.; and Fozzard, H. A. "Accuracy of a Continuous Real-Time ECG Dysrhythmia Monitoring System." Circulation 50 (July 1974):65-72.

Zeelenberg, C.; Deutsch, L. S.; Engelse, W. A. H.; and Corbeij, H. M. A. "Experiences with Implementing ARGUS in a Cardiac Surveillance Unit." Edited by J. H. van Bemmel, and J. L. Williams, Trends in Computer-Processed Electrocardiograms. New York: Elsevier North-Holland Biomedical Press, 1977.